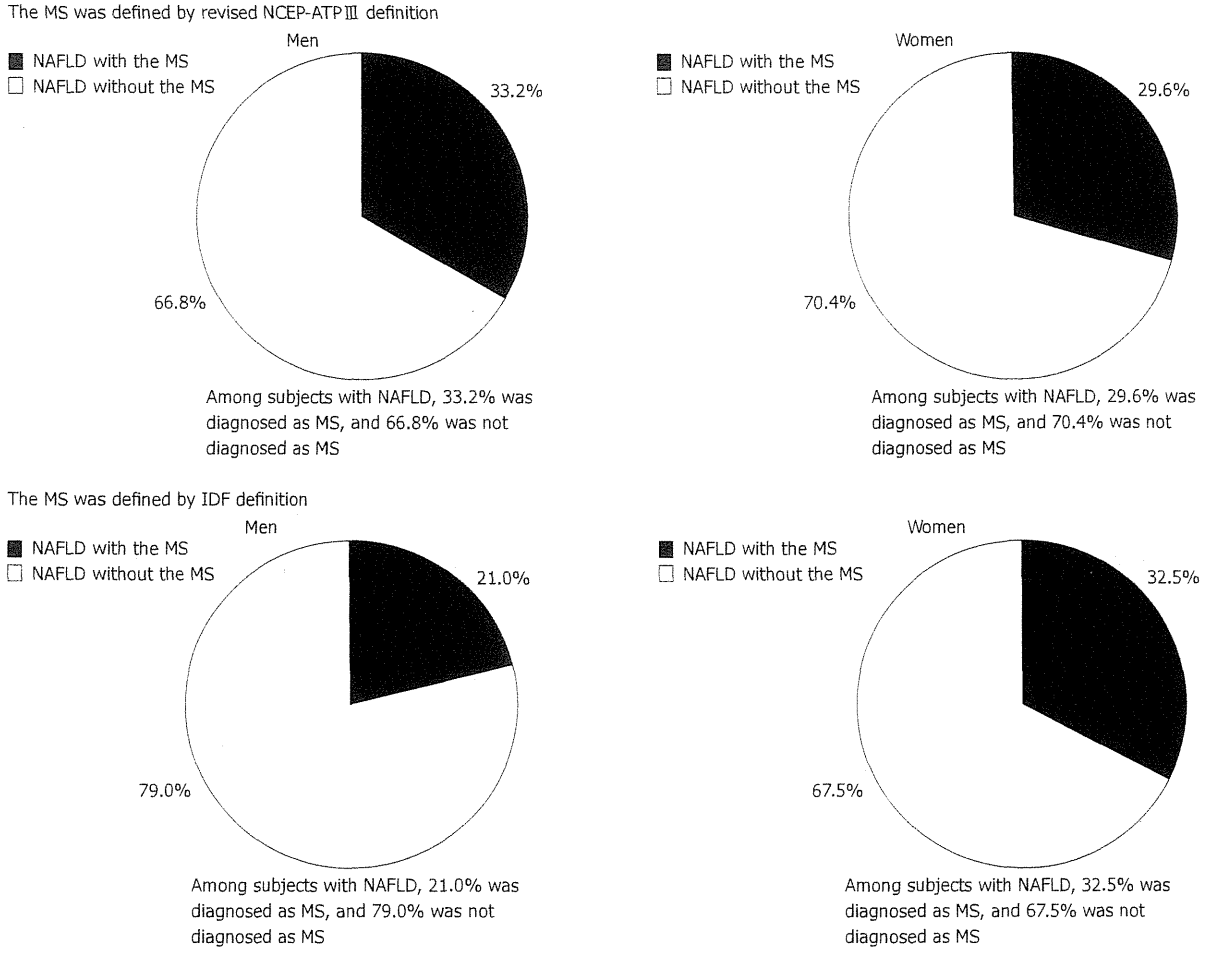

Figure 3 The prevalence of subjects with or without the metabolic syndrome among 1874 men and 514 women with non-alcoholic fatty liver disease. Data was expressed as prevalence (%). The metabolic syndrome (MS) was diagnosed using revised IDF. Among men with NAFLD, 66.8% and 79.0% were not diagnosed with the MS defined by revised NCEP-ATPⅢ definition and revised IDF definition, respectively. In women, 70.4% and 67.5%, respectively, were not diagnosed with the MS by revised NCEP-ATPⅢ definition and revised IDF definition. IDF: International Diabetes Federation; NCEP-ATPⅢ: National Cholesterol Education Program Adult Treatment Panel Ⅲ; NAFLD: Non-alcoholic fatty liver disease.

jects with NAFLD, depending on gender and the criteria used, were diagnosed with the metabolic syndrome. Several previous studies reported how many subjects with NAFLD were diagnosed with the metabolic syndrome, but almost all previous studies were hospital studies. Three population based studies mentioned the prevalence of subjects with NAFLD who were diagnosed with the metabolic syndrome among the general population[8,35,36]. In these studies, the prevalence of the metabolic syndrome among subjects with NAFLD was 17% to 36% depending on gender and the criteria used. The reported prevalence was similar to ours.

There has been no report regarding the sensitivity and specificity of the metabolic syndrome for detecting NAFLD. Among the criteria for metabolic syndrome, the criterion of abdominal circumference had high sensitivity in obese women. However, it had low sensitivity (36.3%) in non-obese women and was very low (5.8%) in non-obese men and low (55.3% in obese men. Other than the criterion of abdominal circumference, none of the sensitivities exceeded 60%. In our study, the specificity of elevated ALT (ALT > 30 IU/L) was 90.6% in men and 98.0% in women. However, the sensitivity was as low as 47.9% in men and 17.7% in women. The specificity of elevated ALT was significantly higher among obese subjects than among non-obese subjects, and sensitivity was higher among obese subjects than among non-obese subjects.

When we investigated the predictability of each component of metabolic syndrome such as abdominal circumference, fasting blood sugar, serum lipid, and blood pressure, each component had high specificity but low sensitivity, similar to elevated ALT. Therefore, we defined it as screening positive for NAFLD, when subjects satisfied at least one criterion of metabolic syndrome; the sensitivity was 84.8% in men and 86.6% in women. Additionally, we defined it as positive when subjects satisfied at least one criterion of metabolic syndrome or elevated ALT. The sensitivity of "at least 1 criterion or elevated ALT" was 90.4% in men and 87.4% in women. However, the specificity of "at least 1 criterion or elevated ALT" was lower -44%-63%.

The result of our study means that we could identify NAFLD effectively in epidemiological study by modifying the usage of the criteria for metabolic syndrome. It is clinically critical evidence that a large part of patients with NAFLD were not diagnosed with the metabolic syndrome, when we used today's definition for the metabolic syndrome. However, our subject population consisted only of Japanese, thus, the generalizability of our study to non-Japanese populations is uncertain. It is one of our study limitations that we used abdominal ultrasonography for diagnosing NAFLD, although the validation ultrasonography had a sensitivity of 91.7% and a specificity of 100%[24].

COMMENTS

Background

It is well known that non-alcoholic fatty liver disease (NAFLD) is associated with the metabolic syndrome and patients with NAFLD tend to also have the metabolic syndrome.

Research frontiers

The impact of overlap between NAFLD and the metabolic syndrome has not been evaluated yet.

Innovations and breakthroughs

It is clinically critical evidence that a large number of patients with NAFLD were not diagnosed with the metabolic syndrome in a healthy Japanese population.

Applications

The authors could identify NAFLD effectively by modifying the usage of the criteria for metabolic syndrome.

Peer review

It is a relatively large population study. The conclusion is consistent with recent observations showing the dissociation between NAFLD and other parameters of metabolic syndrome. The readers of this journal will be interested in the findings of this study.

REFERENCES

1 **Brunt EM**, Janney CG, Di Bisceglie AM, Neuschwander-Tetri BA, Bacon BR. Nonalcoholic steatohepatitis: a proposal for grading and staging the histological lesions. *Am J Gastroenterol* 1999; **94**: 2467-2474

2 **Mulhall BP**, Ong JP, Younossi ZM. Non-alcoholic fatty liver disease: an overview. *J Gastroenterol Hepatol* 2002; **17**: 1136-1143

3 **Bellentani S**, Saccoccio G, Masutti F, Crocè LS, Brandi G, Sasso F, Cristanini G, Tiribelli C. Prevalence of and risk factors for hepatic steatosis in Northern Italy. *Ann Intern Med* 2000; **132**: 112-117

4 **Akbar DH**, Kawther AH. Nonalcoholic fatty liver disease in Saudi type 2 diabetic subjects attending a medical outpatient clinic: prevalence and general characteristics. *Diabetes Care* 2003; **26**: 3351-3352

5 **Gupte P**, Amarapurkar D, Agal S, Baijal R, Kulshrestha P, Pramanik S, Patel N, Madan A, Amarapurkar A. Non-alcoholic steatohepatitis in type 2 diabetes mellitus. *J Gastroenterol Hepatol* 2004; **19**: 854-858

6 **Assy N**, Kaita K, Mymin D, Levy C, Rosser B, Minuk G. Fatty infiltration of liver in hyperlipidemic patients. *Dig Dis Sci* 2000; **45**: 1929-1934

7 **Donati G**, Stagni B, Piscaglia F, Venturoli N, Morselli-Labate AM, Rasciti L, Bolondi L. Increased prevalence of fatty liver in arterial hypertensive patients with normal liver enzymes: role of insulin resistance. *Gut* 2004; **53**: 1020-1023

8 **Hamaguchi M**, Kojima T, Takeda N, Nakagawa T, Taniguchi H, Fujii K, Omatsu T, Nakajima T, Sarui H, Shimazaki M, Kato T, Okuda J, Ida K. The metabolic syndrome as a predictor of nonalcoholic fatty liver disease. *Ann Intern Med* 2005; **143**: 722-728

9 **Radu C**, Grigorescu M, Crisan D, Lupsor M, Constantin D, Dina L. Prevalence and associated risk factors of non-alcoholic fatty liver disease in hospitalized patients. *J Gastrointestin Liver Dis* 2008; **17**: 255-260

10 **McCullough AJ**. The clinical features, diagnosis and natural history of nonalcoholic fatty liver disease. *Clin Liver Dis* 2004; **8**: 521-533, viii

11 **Adams LA**, Angulo P. Recent concepts in non-alcoholic fatty liver disease. *Diabet Med* 2005; **22**: 1129-1133

12 **Marchesini G**, Marzocchi R, Agostini F, Bugianesi E. Nonalcoholic fatty liver disease and the metabolic syndrome. *Curr Opin Lipidol* 2005; **16**: 421-427

13 **Neuschwander-Tetri BA**. Nonalcoholic steatohepatitis and the metabolic syndrome. *Am J Med Sci* 2005; **330**: 326-335

14 **Lavine JE**, Schwimmer JB. Nonalcoholic fatty liver disease in the pediatric population. *Clin Liver Dis* 2004; **8**: 549-558, viii-ix

15 **Marchesini G**, Bugianesi E, Forlani G, Cerrelli F, Lenzi M, Manini R, Natale S, Vanni E, Villanova N, Melchionda N, Rizzetto M. Nonalcoholic fatty liver, steatohepatitis, and the metabolic syndrome. *Hepatology* 2003; **37**: 917-923

16 **Fraser A**, Longnecker MP, Lawlor DA. Prevalence of elevated alanine aminotransferase among US adolescents and associated factors: NHANES 1999-2004. *Gastroenterology* 2007; **133**: 1814-1820

17 **Strauss RS**, Barlow SE, Dietz WH. Prevalence of abnormal serum aminotransferase values in overweight and obese adolescents. *J Pediatr* 2000; **136**: 727-733

18 **Tazawa Y**, Noguchi H, Nishinomiya F, Takada G. Serum alanine aminotransferase activity in obese children. *Acta Paediatr* 1997; **86**: 238-241

19 **Szczepaniak LS**, Nurenberg P, Leonard D, Browning JD, Reingold JS, Grundy S, Hobbs HH, Dobbins RL. Magnetic resonance spectroscopy to measure hepatic triglyceride content: prevalence of hepatic steatosis in the general population. *Am J Physiol Endocrinol Metab* 2005; **288**: E462-E468

20 **Browning JD**, Szczepaniak LS, Dobbins R, Nuremberg P, Horton JD, Cohen JC, Grundy SM, Hobbs HH. Prevalence of hepatic steatosis in an urban population in the United States: impact of ethnicity. *Hepatology* 2004; **40**: 1387-1395

21 **Thamer C**, Tschritter O, Haap M, Shirkavand F, Machann J, Fritsche A, Schick F, Häring H, Stumvoll M. Elevated serum GGT concentrations predict reduced insulin sensitivity and increased intrahepatic lipids. *Horm Metab Res* 2005; **37**: 246-251

22 **Expert Panel on Detection, Evaluation, and Treatment of High Blood Cholesterol in Adults**. Executive Summary of The Third Report of The National Cholesterol Education Program (NCEP) Expert Panel on Detection, Evaluation, And Treatment of High Blood Cholesterol In Adults (Adult Treatment Panel III). *JAMA* 2001; **285**: 2486-2497

23 **Alberti KG**, Zimmet P, Shaw J. Metabolic syndrome--a new world-wide definition. A Consensus Statement from the International Diabetes Federation. *Diabet Med* 2006; **23**: 469-480

24 **Hamaguchi M**, Kojima T, Itoh Y, Harano Y, Fujii K, Nakajima T, Kato T, Takeda N, Okuda J, Ida K, Kawahito Y, Yoshikawa T, Okanoue T. The severity of ultrasonographic findings in nonalcoholic fatty liver disease reflects the metabolic syndrome and visceral fat accumulation. *Am J Gastroenterol* 2007; **102**: 2708-2715

25 **Stone NJ**, Bilek S, Rosenbaum S. Recent National Cholesterol Education Program Adult Treatment Panel III update: adjustments and options. *Am J Cardiol* 2005; **96**: 53E-59E

26 **World Health Organization Western Pacific Region, International Association for the Study of Obesity, International Obesity Task Force**. The Asia-Pacific Perspective: Redefining Obesity and Its Treatment. Sydney: Health Com-

munications, 2000
27 **Marchesini G**, Marzocchi R. Metabolic syndrome and NASH. *Clin Liver Dis* 2007; **11**: 105-117, ix
28 **Jimba S**, Nakagami T, Takahashi M, Wakamatsu T, Hirota Y, Iwamoto Y, Wasada T. Prevalence of non-alcoholic fatty liver disease and its association with impaired glucose metabolism in Japanese adults. *Diabet Med* 2005; **22**: 1141-1145
29 **Fan JG**, Zhu J, Li XJ, Chen L, Lu YS, Li L, Dai F, Li F, Chen SY. Fatty liver and the metabolic syndrome among Shanghai adults. *J Gastroenterol Hepatol* 2005; **20**: 1825-1832
30 **Amarapurkar DN**, Hashimoto E, Lesmana LA, Sollano JD, Chen PJ, Goh KL. How common is non-alcoholic fatty liver disease in the Asia-Pacific region and are there local differences? *J Gastroenterol Hepatol* 2007; **22**: 788-793
31 **Neuschwander-Tetri BA**, Caldwell SH. Nonalcoholic steatohepatitis: summary of an AASLD Single Topic Conference. *Hepatology* 2003; **37**: 1202-1219
32 **Bedogni G**, Miglioli L, Masutti F, Tiribelli C, Marchesini G, Bellentani S. Prevalence of and risk factors for nonalcoholic fatty liver disease: the Dionysos nutrition and liver study. *Hepatology* 2005; **42**: 44-52
33 **Ford ES**, Giles WH, Dietz WH. Prevalence of the metabolic syndrome among US adults: findings from the third National Health and Nutrition Examination Survey. *JAMA* 2002; **287**: 356-359
34 **Kotronen A**, Westerbacka J, Bergholm R, Pietiläinen KH, Yki-Järvinen H. Liver fat in the metabolic syndrome. *J Clin Endocrinol Metab* 2007; **92**: 3490-3497
35 **Sung KC**, Ryan MC, Wilson AM. The severity of nonalcoholic fatty liver disease is associated with increased cardiovascular risk in a large cohort of non-obese Asian subjects. *Atherosclerosis* 2009; **203**: 581-586
36 **Karnikowski M**, Córdova C, Oliveira RJ, Karnikowski MG, Nóbrega Ode T. Non-alcoholic fatty liver disease and metabolic syndrome in Brazilian middle-aged and older adults. *Sao Paulo Med J* 2007; **125**: 333-337

S- Editor Gou SX **L- Editor** O'Neill M **E- Editor** Zhang DN

THE JOURNAL OF BIOLOGICAL CHEMISTRY VOL. 287, NO. 27, pp. 23236–23245, June 29, 2012
Published in the U.S.A.

Anks4b, a Novel Target of HNF4α Protein, Interacts with GRP78 Protein and Regulates Endoplasmic Reticulum Stress-induced Apoptosis in Pancreatic β-Cells*[S]

Received for publication, April 3, 2012, and in revised form, May 11, 2012 Published, JBC Papers in Press, May 15, 2012, DOI 10.1074/jbc.M112.368779

Yoshifumi Sato[‡1], Mitsutoki Hatta[‡1], Md. Fazlul Karim[‡1,2], Tomohiro Sawa[§¶], Fan-Yan Wei[‖], Shoki Sato[‡], Mark A. Magnuson[**], Frank J. Gonzalez[‡‡], Kazuhito Tomizawa[‖], Takaaki Akaike[§], Tatsuya Yoshizawa[‡], and Kazuya Yamagata[‡3]

From the Departments of [‡]Medical Biochemistry and [§]Microbiology, Faculty of Life Sciences, Kumamoto University, Kumamoto 860-8556, Japan, [¶]PRESTO, Japan Science and Technology Agency (JST), 4-1-8 Honcho Kawaguchi, Saitama 332-001, Japan, the [‖]Department of Molecular Physiology, Faculty of Life Sciences, Kumamoto University, Kumamoto, Japan the [**]Department of Molecular Physiology and Biophysics, Vanderbilt University School of Medicine, Nashville, Tennessee 37232, and the [‡‡]Laboratory of Metabolism, NCI, National Institutes of Health, Bethesda, Maryland 20814

Background: Target genes of HNF4α in β-cells are largely unknown.
Results: Expression of Anks4b is decreased in the βHNF4α KO islets. HNF4α activates Anks4b promoter activity. Anks4b binds to GRP78 and regulates sensitivity to ER stress.
Conclusion: HNF4α novel target gene, *Anks4b*, regulates the susceptibility of β-cells to ER stress.
Significance: Anks4b is a novel molecule involved in ER stress.

Mutations of the *HNF4A* gene cause a form of maturity-onset diabetes of the young (MODY1) that is characterized by impairment of pancreatic β-cell function. HNF4α is a transcription factor belonging to the nuclear receptor superfamily (NR2A1), but its target genes in pancreatic β-cells are largely unknown. Here, we report that ankyrin repeat and sterile α motif domain containing 4b (Anks4b) is a target of HNF4α in pancreatic β-cells. Expression of Anks4b was decreased in both βHNF4α KO islets and HNF4α knockdown MIN6 β-cells, and HNF4α activated Anks4b promoter activity. Anks4b bound to glucose-regulated protein 78 (GRP78), a major endoplasmic reticulum (ER) chaperone protein, and overexpression of Anks4b enhanced the ER stress response and ER stress-associated apoptosis of MIN6 cells. Conversely, suppression of Anks4b reduced β-cell susceptibility to ER stress-induced apoptosis. These results indicate that Anks4b is a HNF4α target gene that regulates ER stress in β-cells by interacting with GRP78, thus suggesting that HNF4α is involved in maintenance of the ER.

Hepatocyte nuclear factor (HNF)[4] 4α, a transcription factor belonging to the nuclear receptor superfamily (NR2A1), is expressed in the liver, pancreas, kidney, and intestine (1, 2). HNF4α has multiple functional domains, including the N-terminal A/B domain associated with the transactivation domain (AF-1), a DNA binding C domain, a functionally complex E domain that forms a ligand binding domain, a dimerization interface and transactivation domain (AF-2), and an F domain with a negative regulatory function (3, 4). HNF4α predominantly binds to a 6-bp repeat (AGGTCA) with a 1-bp spacer (mainly A) called direct repeat (DR1).

Maturity-onset diabetes of the young (MODY) is a genetically heterogeneous monogenic disorder that accounts for 2–5% of type 2 diabetes (5). We discovered that mutations of the human *HNF4A* gene cause a particular form of MODY known as MODY1 (6). The primary pathogenesis of MODY1 involves dysfunction of pancreatic β-cells (5). In addition, it has been shown that targeted disruption of HNF4α in pancreatic β-cells leads to defective insulin secretion in mice (7, 8). These findings have demonstrated that HNF4α has an important role in β-cells.

In the liver, HNF4α plays a critical role in nutrient transport and metabolism by regulating numerous target genes, including phosphoenolpyruvate carboxykinase (*PCK1*), glucose-6-phosphatase (*G6PC*), apolipoprotein AII (*APOA2*), and microsomal triglyceride transfer protein (*MTTP*) (9, 10). In contrast, we have little information about the target genes of HNF4α in pancreatic β-cells. Previous *in vitro* studies have suggested that

* This work was supported by a grant-in-aid for scientific research (B), a grant-in-aid for scientific research (S), a grant-in-aid for scientific research in innovative areas, a grant from the Ministry of Health Labour and Welfare, a grant from Takeda Science Foundation, a grant from Novo Nordisk Insulin Research Foundation, a grant from Banyu Life Science Foundation International, and a grant from Japan Diabetes Foundation.
[S] This article contains supplemental Tables 1 and 2 and supplemental Figs. 1–8.
[1] These authors contributed equally to this work.
[2] Supported by a scholarship from the International Priority Graduate Programs Advanced Graduate Courses for International Students, Ministry of Education, Culture, Sports, Science, and Technology in Japan.
[3] To whom correspondence should be addressed. Fax: 81-96-364-6940; E-mail: k-yamaga@kumamoto-u.ac.jp.

[4] The abbreviations used are: HNF, hepatocyte nuclear factor; MODY, Maturity-onset diabetes of the young; ER, endoplasmic reticulum; Anks4b, ankyrin repeat and sterile α motif domain containing 4b; TG, thapsigargin; CHOP, C/EBP homologous protein; C/EBP, CCAAT-enhancer-binding protein; BiP, binding immunoglobulin protein; ESI-Q-TOF, electrospray mass ionization-quadrupole-time-of-flight; KD, knockdown; FL, full-length; MUT, mutant.

HNF4α regulates the expression of pancreatic β-cell genes involved in glucose metabolism, such as insulin (*INS*), solute carrier family 2 (*SLC2A2*), and *HNF1A* (11). However, the expression of these genes was unchanged in the islets of β-cell-specific HNF4α knock-out (βHNF4α KO) mice (7, 8), indicating that such genes are not targets of HNF4α *in vivo*, at least in β-cells.

In the present study, we investigated the mRNA expression profile of βHNF4α KO mice and found that ankyrin repeat and sterile α motif domain containing 4b/harmonin-interacting, ankyrin repeat-containing protein (Anks4b/Harp) is a target of HNF4α in β-cells. We also demonstrated that Anks4b interacts with glucose-regulated protein 78 (GRP78), a major chaperone protein that protects cells from endoplasmic reticulum (ER) stress *in vitro* and *in vivo*. Gain- and loss-of-function studies of Anks4b revealed that it regulates sensitivity to thapsigargin (TG)-induced ER stress and apoptosis in MIN6 β-cell line. Our results suggest that HNF4α plays an important role in the regulation of ER stress and apoptosis in pancreatic β-cells.

EXPERIMENTAL PROCEDURES

Microarray Expression Profiling and HNF4α Motif Scan—Mice were maintained on a 12-h light/12-h dark cycle and allowed free access to food and water. All animal experiments were conducted according to the guidelines of the Institutional Animal Committee of Kumamoto University. Pancreatic islets were isolated from 45-week-old female βHNF4α KO mice (n = 5) and control flox/flox mice (n = 5) by collagenase digestion (12). Total RNA was prepared from the isolated islets with an RNeasy micro kit (Qiagen) according to the manufacturer's instructions, and its quality was confirmed by using an Agilent 2100 Bioanalyzer (Agilent Technologies, Palo Alto, CA). DNA microarray analysis was performed by the Kurabo GeneChip custom analysis service with GeneChip mouse genome 430 2.0 array (Affymetrix Inc., Santa Clara, CA). For identification of potential HNF4α binding sites, 5 kb of the promoter sequence upstream of the transcriptional start site was retrieved from the University of California Santa Cruz Genome Browser, and the sequence was analyzed by using the Transcription Element Search System (TESS) and the HNF4 Motif Finder generated by Sladek and colleagues (38).

Quantitative RT-PCR—Total RNA was extracted using an RNeasy micro kit (catalog number 74004, Qiagen, Valencia, CA) or Sepasol-RNA I super reagent (Nacalai Tesque, Kyoto, Japan). Then 1 μg of total RNA was used to synthesize first-strand cDNA with a PrimeScript RT reagent kit and gDNA Eraser (RR047A, TaKaRa Bio Inc., Shiga, Japan) according to the manufacturer's instructions. Quantitative real-time PCR was performed using SYBR *Premix Ex Taq* II (RR820A, TaKaRa) in an ABI 7300 thermal cycler (Applied Biosystems, Foster City, CA). The specific primers employed are shown in supplemental Table 1. Relative expression of each gene was normalized to that of TATA-binding protein.

Cell Lines and Culture—The MIN6 pancreatic β-cell line was cultured in Dulbecco's modified Eagle's medium (DMEM) containing 25 mM glucose, 15% fetal bovine serum, 0.1% penicillin/streptomycin, and 50 μM 2-mercaptoethanol at 37 °C under 5% CO_2, 95% air (13). HEK293, HeLa, and COS-7 cells were purchased from the American Type Culture Collection (ATCC) and were cultured in DMEM containing 2.5 mM glucose, 10% fetal bovine serum, and 0.02% penicillin/streptomycin.

Western Blotting—Cells were lysed in radioimmunoprecipitation assay buffer (50 mM Tris-HCl (pH 8.0), 150 mM NaCl, 0.1% SDS, 1% Nonidet P-40, 5 mM EDTA, 0.5% sodium deoxycholate, 20 μg/ml Na_3VO_4, 10 mM NaF, 1 mM PMSF, 2 mM DTT, and protease inhibitor mixture (1/100)) from Nacalai Tesque. Total protein was separated by SDS-polyacrylamide gel electrophoresis, transferred to a polyvinylidene fluoride (PVDF) membrane (Immobilon-P; Millipore, Bedford, MA), and probed with primary antibodies. After incubation with the secondary antibodies, the proteins were visualized using Chemi-Lumi One Super (Nacalai Tesque) and a LAS-1000 imaging system (Fuji Film, Tokyo, Japan). The primary antibodies used in this study were as follows: anti-HNF4α (1:1000) (H1415; Perseus Proteomics, Tokyo, Japan), anti-β-actin (1:2000) (A5441; Sigma-Aldrich), anti-harmonin (SAB250188; Sigma-Aldrich) (1:1000), anti-cleaved caspase-3 (Asp-175) (1:1000) (antibody 9661, Cell Signaling), and anti-GRP78 (1:1000) (sc-1051, Santa Cruz Biotechnology or antibody 4332, Cell Signaling).

Anti-Anks4b antiserum was generated by using a peptide that formed the central region of mouse Anks4b protein (amino acid residues 147–344). The nucleotide sequence of the peptide was amplified by PCR using a pair of primers (5′-CGGATCCCCATGAAAGAGTGCGAACGGCTT-3′ and 5′-CGGATCCCCTTACCATTCTACTTCTTCTTC-3′), and then it was subcloned into the pET28C+ vector. After expression in *Escherichia coli* BL21 (DE3), the His-tagged peptide was purified with His binding resin (Novagen) according to the manufacturer's instructions and dialyzed in a buffer containing 20 mM Tris-HCl (pH 8.0) and 500 mM NaCl. Subsequently, this peptide was used to inoculate rabbits for the production of anti-Anks4b antiserum.

Transient Transfection and Luciferase Reporter Assay—The mouse Anks4b promoter containing a putative HNF4α binding site was amplified by PCR using a pair of primers (5′-AGTGGTCATTGCCATGGTTGGT-3′ and 5′-AGGTAGGAGTCTTTGTCTAGGC-3′), and then it was subcloned into the pGL3 basic reporter (Promega). Transcription binding sites were altered by PCR-based mutagenesis to produce an HNF4α binding site mutant (GAACGGGGGCC) and an HNF1α binding site mutant (CTGACCGGCCAG). CD1b-HNF4α is a dominant negative mutant of HNF4α lacking the AF-2 activation domain (3). As described previously (14), the CD1b mutation was introduced by PCR into pcDNA3-HNF4α7 (kindly provided by Dr. Toshiya Tanaka, Tokyo University). The pcDNA3.1-wild-type (WT)-HNF1α and pcDNA3.1-P291fsinsC-HNF1α expression plasmids have been described previously (15). MIN6 cells or HEK293 cells (3×10^5 cells each) were seeded into 24-well plates at 18 h before transfection. Transient transfection was performed using Lipofectamine 2000 (Invitrogen) or X-treme GENE (Roche Applied Science) according to the manufacturer's instructions. At 24 h after transfection, luciferase activity was measured by using a Dual-Luciferase reporter assay system (Promega).

EMSA—A nuclear extract of MIN6 cells was prepared as described previously (16). Then 5 μg of the nuclear extract was incubated with ^{32}P-radiolabeled oligonucleotides containing the HNF4α or HNF1α binding sequence in a mixture containing 10 mM Tris-HCl (pH 7.5), 1% Ficoll, 70 mM KCl, 30 mg/ml BSA, 4.8% glycerol, and 100 μg/ml poly(dI-dC). Next, the DNA-protein complexes were resolved on 4% polyacrylamide gel in 0.5× Tris-borate-EDTA buffer at 120 V for 2 h, after which the dried gel was exposed to a phosphorimaging screen and analyzed with a BAS 2000 (Fuji Film). The oligonucleotide sequences were as follows: wild-type HNF4α binding site (5′-GGCCGGAGTGAACTTTGGCCTGGGGTGATA-3′); mutant HNF4α binding site (5′-GGCCGGAGTGAATGGGAGCCTGGGGTGATA-3′); wild-type HNF1α binding site (5′-CCCCGTCACTGATTAACCAGCCCTGTTGGA-3′); and mutant HNF1α binding site (5′-CCCCGTCACTGACCGGCCAGCCCTGTTGGA-3′). An anti-HNF1 antibody (H205, sc-8986) was used for the supershift assay.

Chromatin Immunoprecipitation—MIN6 cells were fixed in DMEM containing 1% formaldehyde for 10 min at room temperature, and then cross-linking was quenched by placing the cells in 200 mM glycine for 5 min at room temperature. The cells were incubated in Nonidet P-40 buffer (10 mM Tris-HCl (pH 8.0), 10 mM NaCl, 0.5% Nonidet P-40) for 5 min at room temperature and then lysed in SDS lysis buffer (50 mM Tris-HCl (pH 8.0), 1% SDS, 10 mM EDTA) followed by 5-fold dilution in ChIP dilution buffer (50 mM Tris-HCl (pH 8.0), 167 mM NaCl, 1.1% Triton X-100, and 0.11% sodium deoxycholate). Sonication was performed with a Sonifier 150 (Branson). Soluble sheared chromatin (20 μg) was incubated overnight at 4 °C with magnetic beads (Invitrogen Dynabeads protein G) bound to 2 μg of anti-HNF4α antibody (Santa Cruz Biotechnology sc-6556), anti-RNA polymerase II monoclonal antibody (Active Motif), or control IgG (Cell Signaling Technology antibody 2729) followed by sequential washing with low salt radioimmunoprecipitation assay buffer (50 mM Tris-HCl (pH 8.0), 150 mM NaCl, 1 mM EDTA, 0.1% SDS, 1% Triton X-100, and 0.1% sodium deoxycholate), high salt radioimmunoprecipitation assay buffer (50 mM Tris-HCl (pH 8.0), 500 mM NaCl, 1 mM EDTA, 0.1% SDS, 1% Triton X-100, and 0.1% sodium deoxycholate), wash buffer (50 mM Hepes-KOH (pH 7.5), 500 mM LiCl, 1 mM EDTA, 1% Nonidet P-40, and 0.7% sodium deoxycholate), and Tris-EDTA. Then immune complexes were eluted from the magnetic beads by incubation with ChIP direct elution buffer (50 mM Tris-HCl (pH 8.0), 10 mM EDTA, and 1% SDS) for 20 min at 65 °C. For reverse cross-linking, the eluate was incubated overnight at 65 °C, and then DNA fragments were purified by using a PCR purification kit (Qiagen). PCR was performed to identify Anks4b promoter fragments in the immunoprecipitated DNA using a pair of primers (5′-TTCACCACACTCATGACACACC-3′ and 5′-AGGTAGGAGTCTTTGTCTAGGC-3′).

GST Pulldown Assay—Mouse Anks4b cDNA was amplified by PCR using a pair of primers (5′-CGGATCCCCATGTCTACCCGCTATCACCAA-3′ and 5′-CGGATCCTTAGAGGCTGGTGTCAACCAACT-3′) and was subcloned into the pGEX4T2 vector (GE Healthcare). Anks4b deletion mutants (N-Anks4b (amino acid residues 1–126), M-Anks4b (amino acid residues 127–345), and C-Anks4b (amino acid residues 346–423)) were also generated by PCR and subcloned into the pGEX4T3 vector (GE Healthcare). GST-Anks4b proteins were expressed in *E. coli* BL21 (DE3) and purified with glutathione-Sepharose 4B beads (GE Healthcare). GST or GST fusion proteins (20 μg) immobilized on glutathione-Sepharose beads were incubated with 500 μg of mouse liver lysate. After binding overnight at 4 °C, the beads were washed with lysis buffer containing 10 mM Tris-HCl (pH 7.4), 150 mM NaCl, 1% Nonidet P-40, 1 mM EDTA, 10 mM NaF, 10 mM $Na_4P_2O_7$, 1 mM PMSF, and protease inhibitor mixture (Nacalai Tesque). Then the bound proteins were separated by SDS-PAGE.

Proteomic Identification of Anks4b-interacting Proteins—Silver-stained gels were subjected to in-gel digestion followed by extraction of peptides and proteomic analysis by LC-MS/MS. Gel digestion and peptide extraction were performed as reported previously (17). The peptide samples thus obtained were analyzed in an ESI-Q-TOF tandem mass spectrometer (6510; Agilent) with an HPLC chip-MS system, consisting of a nano pump (G2226; Agilent) with a four-channel microvacuum degasser (G1379B; Agilent), a microfluidic chip cube (G4240; Agilent), a capillary pump (G1376A; Agilent) with degasser (G1379B; Agilent), and an autosampler with thermostat (G1377A; Agilent). All modules were controlled by MassHunter software (version B.02.00; Agilent). A microfluidic reverse-phase-HPLC chip (Zorbax 300SB-C18; 5-μm particle size, 75-mm inner diameter, and 43 mm in length) was used for separation of peptides. The nano pump was employed to generate gradient nano flow at 600 nl/min, with the mobile phase being 0.1% formic acid in MS-grade water (solvent A) and 0.1% formic acid in acetonitrile (solvent B). The gradient was 5–75% solvent B over 9 min. A capillary pump was used to load samples with a mobile phase of 0.1% formic acid at 4 μl/min. The Agilent ESI-Q-TOF was operated in the positive ionization mode (ESI+), with an ionization voltage of 1,850 V and a fragmentor voltage of 175 V at 300 °C. Fragmentation of protonated molecular ions was conducted in the auto-MS/MS mode, starting with a collision energy voltage of 3 V that was increased by 3.7 V per 100 Da. The selected m/z ranges were 300–2,400 Da in the MS mode and 59–3,000 Da in the MS/MS mode. The data output consisted of one full mass spectrum (with three fragmentation patterns per spectrum) every 250 ms. The three highest peaks of each MS spectrum were selected for fragmentation. Mass lists were created in the form of Mascot generic files and were used as the input for Mascot MS/MS ion searches of the National Center for Biotechnology Information nonredundant (NCBI nr) database using the Matrix Science Web server Mascot version 2.2. Default search parameters were as follows: enzyme, trypsin; maximum missed cleavage, 1; variable modifications, carbamidomethyl (Cys); peptide tolerance, ± 1.2 Da; MS/MS tolerance, ± 0.6 Da; peptide charge, 2+ and 3+; instrument, ESI-Q-TOF. For positive identification, the result of ($-10 \times \log(p)$) could not exceed the significance threshold ($p < 0.05$).

Immunoprecipitation—Mouse Anks4b cDNA was amplified by PCR using a pair of primers (5′-CGGATCCCCATGTCTACCCGCTATCACCAA-3′ and 5′-CGGATCCTTAGAGGCTGGTGTCAACCAACT-3′) and was subcloned in-frame

into the pcDNA3-HA and pcDNA3-FLAG expression vectors. The GRP78 expression vector (pCMV-BiP-Myc-KDEL-wt) was a gift from Dr. Ron Prywes (Addgene plasmid 27164). After transfection into COS-7 cells, the cells were lysed in immunoprecipitation buffer (20 mM Tris-HCl (pH 7.4), 175 mM NaCl, 2.5 mM $MgCl_2$, 0.05% Nonidet P-40, 1 mM PMSF, and protease inhibitor mixture (Nacalai Tesque)) and incubated on ice for 30 min. Then 700 μg of cell lysate and FLAG tag antibody beads (Wako) were mixed and stirred at 4 °C for 18 h. After washing with immunoprecipitation buffer, proteins were eluted by using DYKDDDDK peptide (Wako). A sample of the eluate and 2% of the cell lysate (from before processing) were subjected to Western blotting analysis.

Immunocytochemistry—Both the pcDNA3-HA-Anks4b and the pCMV-BiP-Myc-KDEL-wt vectors were transfected into HeLa, COS-7, and MIN6 cells with X-treme GENE (Roche Diagnostics) for 24 h. Then the cells were fixed in 10% neutralized formalin and permeabilized with 0.1% Triton X-100, 3% BSA/PBS. Monoclonal rat anti-HA antibody (1:400) (clone 3F10, Roche Applied Science) and mouse anti-c-Myc antibody (1:400) (Wako) were used as the primary antibodies, whereas Alexa Fluor 568 goat anti-rat IgG (Invitrogen) and Alexa Fluor 488 goat anti-mouse IgG (Invitrogen) were used as the secondary antibodies. Immunofluorescence was detected under a laser scanning confocal microscope (FV-1000, Olympus, Tokyo, Japan).

Retrovirus Infection—Mouse Anks4b and human HNF4α7 cDNAs were subcloned into the pMXs-puro retrovirus vector for overexpression (18). Specific shRNA sequences for mouse HNF4α (5′-CCAAGAGCTGCAGATTGAT-3′) and Anks4b (5′-GAAGAAGACTCATTTCCAA-3′) were designed using the Clontech RNAi target sequence selector. Oligonucleotides encoding shRNA were synthesized and cloned into the pSIREN-RetroQ retroviral shRNA expression vector (Clontech). Then the pMXs-Anks4b, pMXs-HNF4α7, and empty pMXs vectors were transfected into Plat-E cells using FuGENE6 (Roche Applied Science, Mannheim, Germany). For knockdown experiments, transfection was done with pSIREN-RetroQ-Anks4b, pSIREN-RetroQ-HNF4α, and the negative control pSIREN-RetroQ vector. MIN6 cells were infected with the retroviruses and selected by incubation with puromycin (5 μg/ml) (12).

Flow Cytometric Analysis—An annexin V-FITC apoptosis detection kit (BioVision Research Products, Mountain View, CA) was used for the apoptosis assay according to the manufacturer's instructions. MIN6 cells were cultured in DMEM for 30 h with or without 1 μM thapsigargin (Nacalai Tesque). After incubation in trypsin/EDTA for 10 min at 37 °C, cells were centrifuged at 6,000 rpm for 10 min. The pellet was resuspended in 1×resuspension buffer, and the cells were stained with annexin V-FITC antibody. After incubation for 5 min at room temperature in the dark, stained cells were analyzed using a FACSCalibur (BD Biosciences) and FlowJo software (Tomy Digital Biology, Tokyo, Japan).

Statistical Analysis—Statistical analyses were performed using Statview J-5.0 software (SAS Institute, Cary, NC). The significance of differences was assessed with the unpaired *t* test, and $p < 0.05$ was considered to indicate statistical significance.

RESULTS

Anks4b Is a Novel Target of HNF4α—To identify target genes of HNF4α in pancreatic β-cells, DNA microarray analysis was performed using islets from βHNF4α KO mice and control mice. Body weight and blood glucose levels were similar for these two strains of mice (body weight was 32.7 ± 1.7 g ($n = 5$) *versus* 34.1 ± 1.9 g ($n = 5$) and random blood glucose was 128 ± 27 mg/dl ($n = 5$) *versus* 114 ± 24 mg/dl ($n = 5$) for βHNF4α KO *versus* control mice). Microarray analysis identified 56 up-regulated genes (signal log ratio ≥2) and 100 down-regulated genes (signal log ratio ≤−1.5) in βHNF4α KO islets (supplemental Table 2). Expression of the majority of the genes known to be involved in glucose metabolism was unchanged. To validate these results, expression of mRNA for genes randomly chosen from both the down-regulated and the up-regulated groups was assessed by quantitative real-time PCR in an independent group of 12-week-old male mice. As a result, differential expression of most genes was confirmed (Fig. 1*A* and supplemental Fig. 1). Gupta *et al.* (19) reported that ST5, a regulator of ERK activation, is a direct target of HNF4α in β-cells. Expression of ST5 mRNA was reduced by 24.6% in βHNF4α KO islets (supplemental Fig. 2).

Next, we performed a computational scan of the HNF4α binding motif in the down-regulated genes. This identified 22 high affinity HNF4α binding sequences in the mouse promoter. In 3 out of 22 genes, the HNF4 motif was also conserved in the corresponding human genome. These three genes encoded *Anks4b*, guanylate cyclase 2c (*Gucy2c*), and peroxisome proliferator-activated receptor γ coactivator-1α (*Ppargc1a*). Quantitative real-time PCR analysis confirmed a significant decrease of Anks4b expression in the islets of 12-week-old βHNF4α KO mice (17.3% of the control level, $p < 0.01$) (Fig. 1*B*). In contrast, the reduction of Gucy2c mRNA expression was marginal (21.7% of the control level, $p = 0.06$), and *Ppargc1a* mRNA levels were unchanged. The difference of sex and age of mice or different detection systems might have contributed to the different results. To elucidate the direct effect of HNF4α on the expression of these three genes, we established MIN6 β-cells that stably expressed HNF4α-specific shRNA (HNF4α KD-MIN6) by retroviral infection. Suppression of endogenous HNF4α was confirmed at both the mRNA and the protein levels (Fig. 1*C*). Decreased expression of *Anks4b*, *Gucy2c*, and *Ppargc1a* was found in HNF4α KD-MIN6 cells (Fig. 1*D*). Because *Anks4b* gene expression was most markedly decreased in both βHNF4α KO islets and HNF4α KD-MIN6 cells (35.2% of the control level, $p < 0.001$), we focused on Anks4b for further investigation.

Screening of the promoter region of the mouse Anks4b gene by using a genomic databank revealed an HNF4α binding site (nucleotides −108 to −120 relative to the translation start codon when A is designated as +1). We cloned a 190-bp promoter region upstream of a luciferase reporter gene and co-expressed it with the HNF4α expression vector in HEK293 cells. Induction of HNF4α7 (an isoform expressed in pancreatic β-cells (4)) increased Anks4b promoter activity in a concentration-dependent manner (Fig. 2*A*), whereas overexpression of the HNF4α mutant lacking AF-2 had no effect (Fig. 2*B*). When

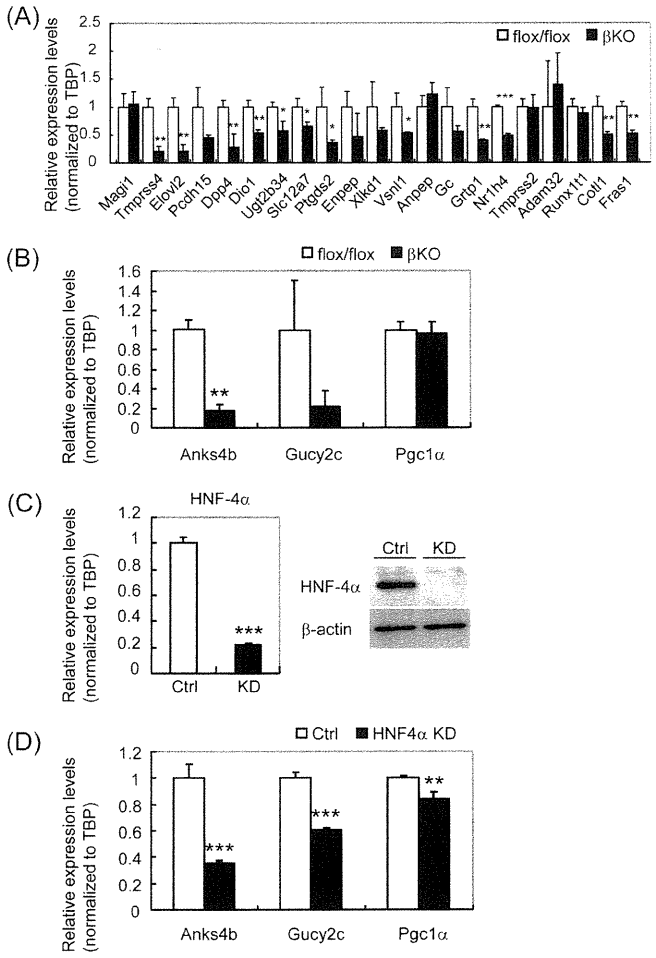

FIGURE 1. **Gene expression in the islets of βHNF4α KO mice and HNF4α knockdown MIN6 cells.** *A*, quantitative RT-PCR analysis of genes randomly chosen from those in supplemental Table 1 using flox/flox control (*white bar*) and βHNF4α KO islets (*black bar*, male, 12 week, $n = 4$). Expression of each gene was normalized for that of TATA-binding protein (*TBP*). *B*, expression of *Anks4b*, *Gucy2c*, and *Ppargc1a* in βHNF4α KO islets. Decreased expression of Anks4b was confirmed by quantitative RT-PCR. *C*, HNF4α mRNA (*left*) and HNF4α protein (*right*) in control (*Ctrl*, *white bar*) and HNF4α knockdown MIN6 cells (*KD*, *black bar*) were evaluated by quantitative PCR ($n = 4$) and Western blotting, respectively. β-Actin was used as the loading control. *D*, expression of *Anks4b*, *Gucy2c*, and *Ppargc1a* was significantly decreased in HNF4α KD-MIN6 cells. The mean ± S.D. for each group is shown (*, $p < 0.05$, **, $p < 0.01$, ***, $p < 0.001$).

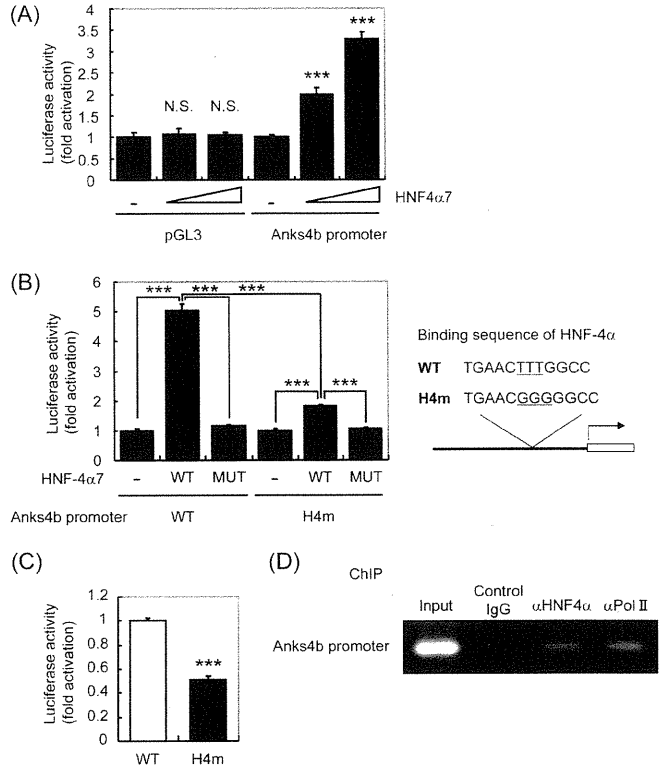

FIGURE 2. **Transcriptional regulation of Anks4b by HNF4α.** *A*, HEK293 cells were cotransfected with the pcDNA3-HNF4α7 expression vector (0–75 ng), as well as 50 ng of pGL3 basic or pGL3-Anks4b reporter and 25 ng of pRL-TK. *B*, HEK293 cells were cotransfected with 50 ng of pcDNA3-wild-type-HNF4α7 (WT) or pcDNA3-mutant (MUT) HNF4α7, as well as 50 ng of pGL3-Anks4b reporter (WT and MUT) and 25 ng of pRL-TK. *C*, MIN6 cells were transfected with pGL3-Anks4b reporter (WT and MUT) and 25 ng of pRL-TK. The mean ± S.D. for each group ($n = 3$) is shown (***, $p < 0.001$). *N.S.*, not significant. *D*, chromatin immunoprecipitation assay with MIN6 cells. Interaction of HNF4α with the promoter of Anks4b was observed. *αPol II*, RNA polymerase II antibody.

the putative HNF4α binding site in the Anks4b promoter was subjected to mutation (H4m), transcriptional activation by HNF4α7 was significantly reduced by 64.0% ($p < 0.001$) (Fig. 2*B*). Disruption of the HNF4α binding site was also associated with a 48.5% reduction of promoter activity in MIN6 cells ($p < 0.001$) (Fig. 2*C*). To assess the binding of HNF4α to the Anks4b promoter, a chromatin immunoprecipitation (ChIP) assay was performed using MIN6 cells. This assay revealed binding of HNF4α to the Anks4b promoter of MIN6 cells (Fig. 2*D*). Specific binding of HNF4α to the putative binding site was also demonstrated by the electrophoretic mobility shift assay (EMSA) (supplemental Fig. 3). Thus, both *in vivo* and *in vitro* data indicated that Anks4b is a direct target of HNF4α in β-cells.

HNF4α and HNF1α Synergistically Activate Transcription of Anks4b—HNF1α is a homeodomain-containing transcription factor that is also expressed in the liver, kidney, intestine, and pancreas (20). Mutation of the *HNF1A* gene causes another type of MODY known as MODY3 (21). In addition to the binding site for HNF4α, we also found an HNF1α binding consensus sequence in the Anks4b promoter (Fig. 3*A*). Therefore, we examined the role of HNF1α in Anks4b gene transcription. First, binding of HNF1α to the Anks4b gene was examined by EMSA with MIN6 nuclear extracts and a probe corresponding to the HNF1α binding site (Fig. 3*B*). The probe shifted after the addition of nuclear extracts (*lane 2*), and its binding was blocked by the addition of a 30-fold excess of unlabeled oligonucleotide (*lane 3*). Specificity of HNF1α binding was assessed by supershifting the DNA-HNF1α complex using HNF1α antibody (*lane 5*), indicating that HNF1α also binds directly to the Anks4b promoter. To examine the influence of HNF1α on Anks4b gene expression, we next performed a reporter gene assay. WT-HNF1α caused a dose-dependent increase of Anks4b promoter activity (Fig. 3*C*). Interestingly, Anks4b mRNA expression was decreased in HNF1α KO islets according to the results of DNA microarray analysis (22). Taken together, these results suggested that Anks4b is a target of

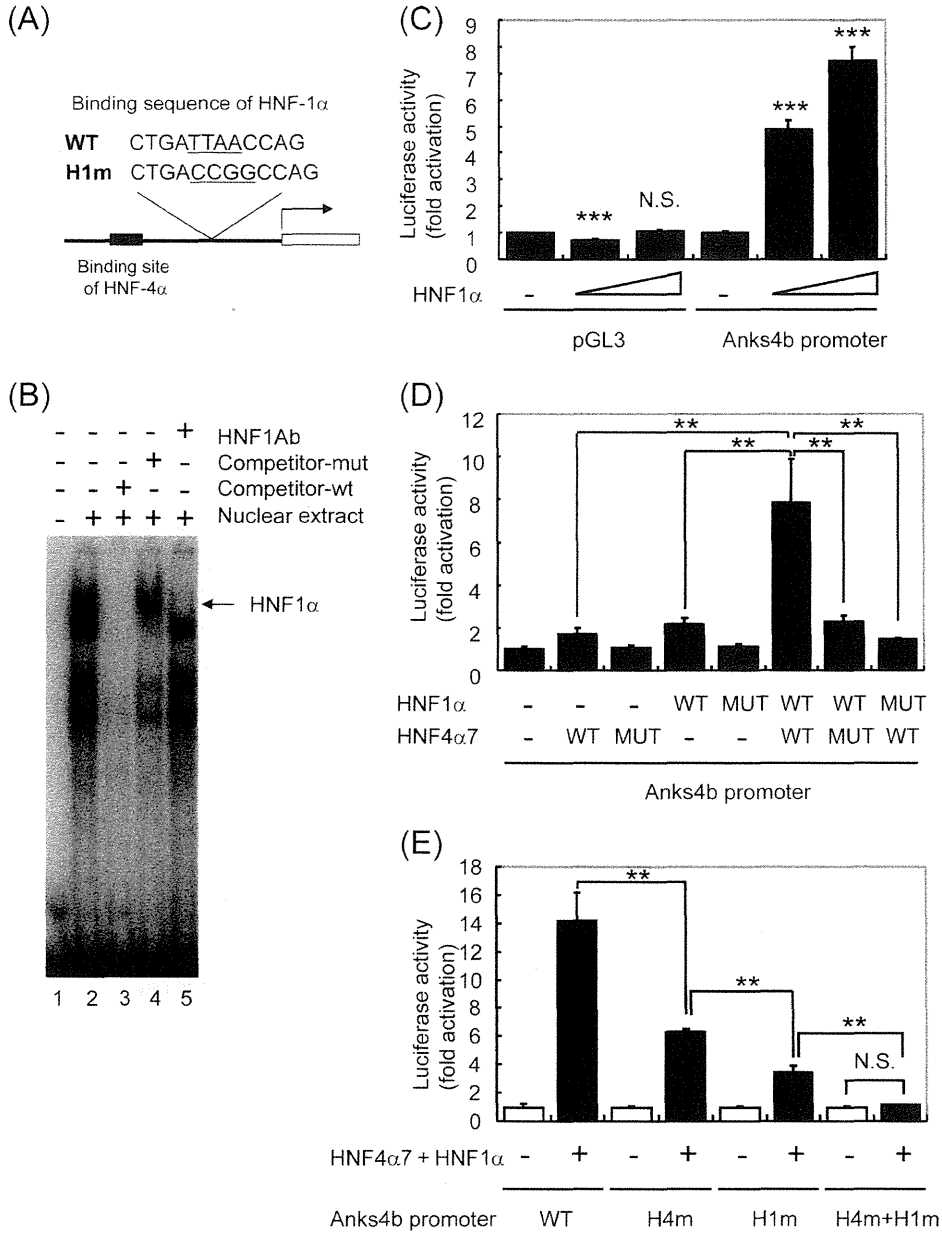

FIGURE 3. **Synergistic activation of Anks4b transcription by HNF4α and HNF1α.** *A*, DNA sequences of the promoter region of the mouse and human Anks4b genes. The putative HNF4α and HNF1α binding sites are shown. *B*, EMSA analysis of the HNF1α binding site in the Anks4b gene. DNA binding was tested using nuclear extracts from MIN6 cells. *C*, HEK293 cells were cotransfected with the pcDNA3.1-HNF1α expression vector (0–75 ng), as well as 50 ng of pGL3 basic or pGL3-Anks4b reporter and 25 ng of pRL-TK. *D*, HEK293 cells were cotransfected with 10 ng of pcDNA3.1-HNF1α (WT or MUT) and 10 ng of pcDNA3-HNF4α7 (WT or MUT), as well as 50 ng of pGL3-Anks4b reporter and 5 ng of pRL-TK. *E*, HEK293 cells were cotransfected with pcDNA3.1-HNF1α and pcDNA3-HNF4α7 as well as 50 ng of pGL3-Anks4b reporter (WT or MUT). *H4m*, mutation of the HNF4α binding site; *H1m*, mutation of the HNF1α binding site. *H4m+H1m*, mutation of both binding sites. The mean ± S.D. for each group ($n = 3$) is shown (**, $p < 0.01$, ***, $p < 0.001$). *N.S.*, not significant.

HNF1α as well as HNF4α. Because it has been reported that HNF4α and HNF1α cooperatively activate target genes that have binding sites for both HNFs in the promoter region (23, 24), we examined the influence on Anks4b gene expression of interaction between HNF4α and HNF1α. When an Anks4b reporter construct was cotransfected into HEK293 cells with 10 ng of HNF1α or HNF4α expression plasmid, the reporter gene was activated by 2.2- and 1.7-fold, respectively (Fig. 3*D*). In contrast, there was a dramatic increase of promoter activity (7.9-fold) when both constructs were cotransfected simultaneously (Fig. 3*D*). Mutation of either HNF1α or HNF4α markedly suppressed this response (Fig. 3*D*). Synergistic activation of Anks4b promoter activity was significantly suppressed by disruption of either the HNF4α binding site (H4m) or the HNF1α binding site (H1m), and activation was completely abolished by both H4m and H1m (Fig. 3*E*). Taken together, these results indicate that Anks4b promoter activity is synergistically regulated by both HNF4α and HNF1α.

Anks4b Interacts with GRP78 Both in Vitro and in Vivo—Anks4b is a scaffold protein with three ankyrin repeats and a sterile α motif domain that was identified as harmonin-interacting protein (25), although its function is completely

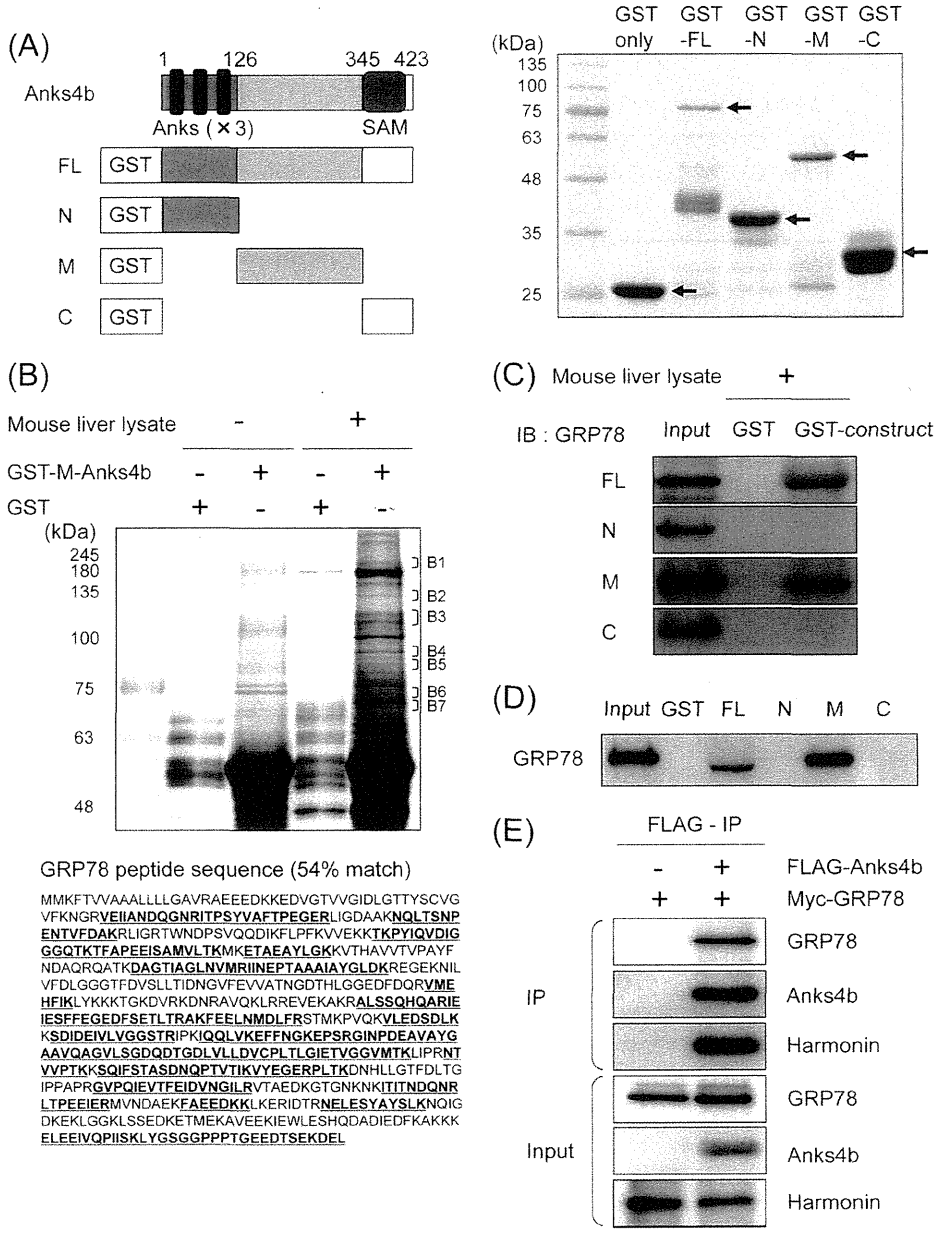

FIGURE 4. **Interaction of Anks4b and GRP78 *in vitro* and *in vivo*.** *A*, schematic representation of full-length Anks4b (*FL*) and deletion mutants of Anks4b (N-Anks4b (*N*), M-Anks4b (*M*), and C-Anks4b (*C*)) and expression of GST-Anks4b fusion proteins (Coomassie Brilliant Blue staining). *SAM*, sterile α motif. *B*, purification of proteins interacting with Anks4b. The GST pulldown assay using M-Anks4b was performed with mouse liver lysates. Eluted proteins were resolved by SDS-PAGE and then silver-stained. Seven regions (*B1–B7*) were excised for mass spectrometry. GRP78 residues were detected by mass spectrometry (*bold* and *underlined letters*). *C* and *D*, interaction of Anks4b and GRP78 *in vitro*. After the pulldown assay using mouse liver lysates (*C*) or MIN6 lysates (*D*), binding of GRP78 with FL- and M-Anks4b was detected by Western blotting (*IB*). *E*, interaction of Anks4b and GRP78 *in vivo*. COS-7 cells were transfected with the pCMV-Bip/GRP78-Myc-KDEL-wt or pCMV-Bip/GRP78-Myc-KDEL-wt and pcDNA3-FLAG-Anks4b expression vectors. Immunoprecipitation (*IP*) was performed with FLAG resin and 700 μg of COS-7 cell lysate.

unknown. To elucidate the role of Anks4b in β-cells, we searched for molecules that interacted with full-length Anks4b (FL) and with its deletion mutants (N-, M-, and C-Anks4b) (Fig. 4*A*) by performing a GST pulldown assay of mouse liver lysates (Fig. 4*B* and supplemental Fig. 4). We found a protein of ~75 kDa that specifically precipitated with GST-M-Anks4b (B6), and it was identified as GRP78/binding immunoglobulin protein (BiP) by mass spectrometry (Fig. 4*B*). GRP78 is an ER-localized chaperone protein that is induced by the unfolded protein response in response to ER stress (26, 27). Binding of GRP78 to GST-FL-Anks4b and GST-M-Anks4b, but not to GST, GST-N-Anks4b, or C-Anks4b, was confirmed by Western blotting using a specific antibody for GRP78 (Fig. 4*C*), suggesting that GRP78 bound to the middle region of Anks4b. GST pulldown experiments using MIN6 cell lysates also demonstrated binding of GRP78 to Anks4b (Fig. 4*D*).

Subsequently, we evaluated the interaction between Anks4b and GRP78 in cultured cells. COS-7 cells were transfected with the Myc-GRP78 expression plasmid alone or with Myc-GRP78 plus FLAG-tagged wild-type Anks4b expression plasmids, and

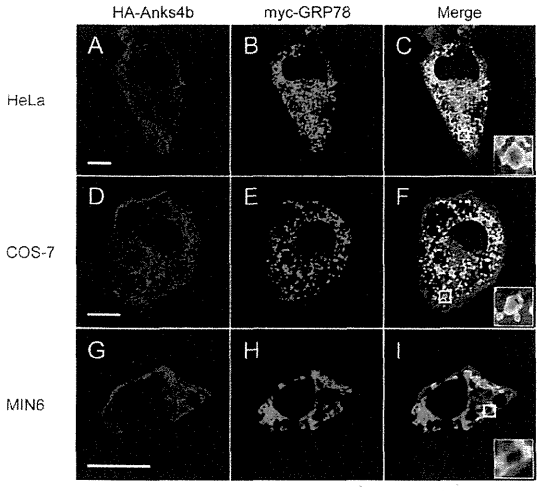

FIGURE 5. **Intracellular localization of Anks4b adjacent to the ER membrane.** *A–I*, HeLa (*A–C*), COS-7 (*D–F*), and MIN6 (*G–I*) cells were cotransfected with the pcDNA3-HA-Anks4b and pCMV-Bip/GRP78-Myc-KDEL-wt expression vectors. Cells were double-stained with anti-HA antibody (Alexa Fluor 563, *red*) and anti-Myc antibody (Alexa Fluor 488, *green*). DAPI (*blue*) was used for nuclear staining. *Insets* represent higher magnifications of the *boxed regions* in *C* (×18), *F* (×13), and *I* (×8). *Scale bar* = 10 μm.

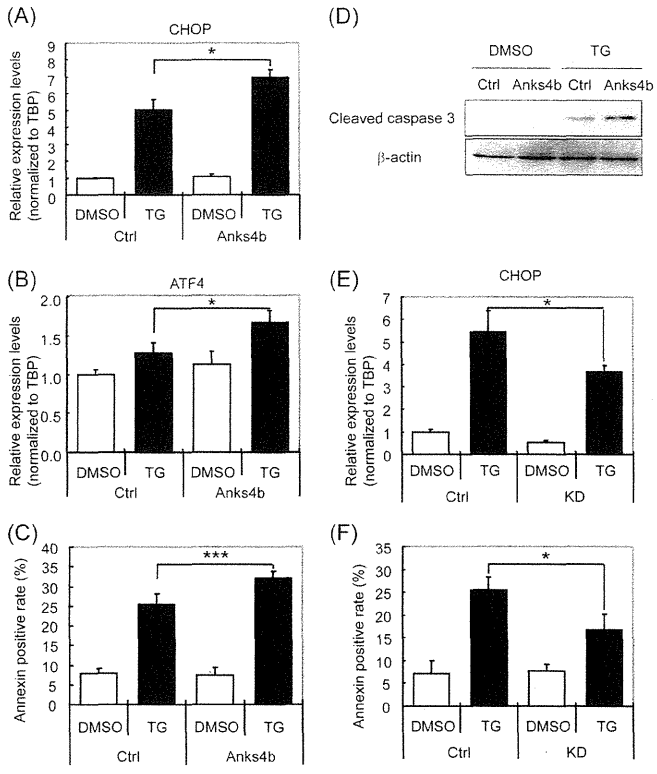

FIGURE 6. **Regulation of ER stress-mediated apoptosis by Anks4b.** *A* and *B*, MIN6 cells overexpressing Anks4b were cultured in the absence or presence of 1 μM thapsigargin for 20 h, and then quantitative RT-PCR was performed. *TBP*, TATA-binding protein. *DMSO*, dimethyl sulfoxide; *Ctrl*, control. *C*, MIN6 cells overexpressing Anks4b were cultured in the absence or presence of 1 μM thapsigargin for 30 h, and the percentage of annexin V-positive cells was analyzed by flow cytometry. *D*, Western blotting of cleaved caspase-3 after treatment with 1 μM thapsigargin for 20 h. *E*, Anks4b knockdown MIN6 cells were cultured for 20 h with 1 μM thapsigargin, and then quantitative RT-PCR was performed. *F*, annexin V-positive cells were analyzed after treatment of Anks4b knockdown MIN6 cells with 1 μM thapsigargin for 30 h. The mean ± S.D. for each group ($n = 4$) is shown (*, $p < 0.05$, **, $p < 0.01$, ***, $p < 0.001$).

cell lysates were immunoprecipitated with FLAG resin. As shown in Fig. 4*E*, FLAG-Anks4b was able to coimmunoprecipitate GRP78 as well as harmonin, a protein that was previously found to interact with Anks4b (25). These results indicated that Anks4b binds to GRP78 in cells.

Anks4b Colocalizes with GRP78 in the Endoplasmic Reticulum—We next investigated the intracellular localization of Anks4b. HA-tagged Anks4b and Myc-tagged GRP78 constructs were cotransfected into HeLa cells, and an immunofluorescence study was performed. HA staining (Anks4b, *red*) revealed a reticular pattern in the cytoplasm, but no signals were detected in the nucleus (Fig. 5*A*). Double staining for Anks4b and GRP78 (Myc, *green*) as a marker for the ER revealed that both signals were frequently colocalized (Fig. 5, *B* and *C*). In contrast, Anks4b staining did not overlap with MitoTracker, a specific marker for the mitochondria (supplemental Fig. 5). A similar staining pattern was also detected in COS-7 cells and MIN6 cells (Fig. 5, *D–I*). These findings were further evidence that Anks4b interacts with GRP78. Notably, Anks4b staining was detected at the periphery of the ER lumen (Fig. 5, *C*, *F*, and *I*, *inset*), suggesting that it was localized adjacent to the ER membrane.

Anks4b Regulates Apoptosis in Response to ER Stress—GRP78 is a major chaperone protein that protects cells from ER stress, and overexpression of GRP78 reduces ER stress-mediated apoptosis by attenuating the expression of C/EBP homologous protein (CHOP) (28, 29). Accordingly, detection of an interaction between Anks4b and GRP78 prompted us to investigate the role of Anks4b in both ER stress and apoptosis. TG causes ER stress by preventing calcium uptake from the cytoplasm into the ER (30), and treatment of MIN6 cells with 1 μM TG for 20 h increased the expression of the ER stress-related genes (ATF4, spliced XBP1, and CHOP) (data not shown). First, we examined the effect of Anks4b overexpression on MIN6 cells (supplemental Fig. 6). Anks4b overexpression did not affect CHOP gene expression in the absence of TG, but TG-induced CHOP expression was significantly increased (1.4-fold, $p < 0.05$) (Fig. 6*A*). TG-induced ATF4 expression was also significantly augmented in Anks4b-overexpressing MIN6 cells (1.3-fold, $p < 0.05$) (Fig. 6*B*). Furthermore, the number of annexin V-positive apoptotic cells was increased by overexpression of Anks4b (1.3-fold, $p < 0.001$) (Fig. 6*C*). Augmentation of apoptosis was also observed in MIN6 cells overexpressing HNF4α7 (supplemental Fig. 7). Activation of caspase-3 mediates the induction of apoptosis downstream of CHOP (31), and activated (cleaved) caspase-3 protein expression was increased when Anks4b-overexpessing MIN6 cells were treated with TG (Fig. 6*D*).

Next, we examined the effect of knockdown of Anks4b in MIN6 cells (supplemental Fig. 8). Suppression of endogenous Anks4b mRNA by shRNA in MIN6 (reduced to 40.5% of the control level) did not affect CHOP gene expression in the absence of TG, but TG-induced CHOP expression was significantly reduced by 32.1% ($p < 0.05$) (Fig. 6*E*). In addition, flow cytometric analysis using annexin V revealed that TG-induced apoptosis was also decreased by suppression of Anks4b (Fig. 6*F*). Collectively, these findings indicate that Anks4b promotes the induction of ER stress and apoptosis by TG in MIN6 cells.

DISCUSSION

HNF4α plays an important role in pancreatic β-cells, and mutation of this gene causes MODY1 (6). However, there has been little information available about the target genes of HNF4α in β-cells. We and others have previously reported that most of the genes involved in glucose metabolism, including *Slc2a2*, *Gck*, *Kcnj11*, *Abcc8*, and *Ins*, are not differentially expressed in βHNF4α KO islets (7, 8, 19). The present large scale expression profiling analysis also demonstrated that expression of genes known to be involved in insulin secretion was largely unchanged in HNF4α deficient islets. Like HNF4α, mutation of the HNF1α gene also causes a form of MODY (MODY3), which is characterized by β-cell dysfunction (21). Expression of many genes involved in insulin secretion, including *Slc2a2*, *Pklr*, and *Tmem27*, is decreased in HNF1α KO islets (22, 32, 33). Thus, the gene expression pattern of HNF4α KO islets differs markedly from that of HNF1α KO islets.

In the present study, we found that Anks4b gene expression was markedly reduced in both βHNF4α KO islets and HNF4α KD-MIN6 cells. Reporter gene assays and ChIP analysis demonstrated that HNF4α bound to a conserved HNF4 binding motif and activated transcription, thus indicating that Anks4b is a direct target of HNF4α in β-cells. In addition to the pancreatic islets, Anks4b is also expressed in the liver, kidney, small intestine, and colon (25). This distribution of expression is very similar to that of HNF4α, suggesting that HNF4α plays a role in Anks4b gene transcription in these tissues. Furthermore, we found that Anks4b gene expression was also regulated by HNF1α. Cotransfection of HNF4α and HNF1α dramatically stimulated promoter activity when compared with the sum of the effects of each transcription factor acting separately (Fig. 3*D*). Recently, Boj *et al.* (34) reported that HNF4α and HNF1α regulate common target genes through interdependent regulatory mechanisms. Although the mechanism of the functional interaction between HNF4α and HNF1α is still unclear, our results indicate that Anks4b gene expression is another example of such interdependent regulation.

Anks4b was originally identified as harmonin (the gene responsible for Usher deafness syndrome type 1C)-interacting protein, but its function is unknown. In this study, we showed that Anks4b binds to GRP78, a major ER chaperone protein. We also found that Anks4b knockdown significantly inhibited TG-induced CHOP expression and apoptosis in MIN6 cells, whereas Anks4b overexpression enhanced TG-induced CHOP expression and apoptosis, strongly suggesting a direct role of Anks4b in increasing the susceptibility of β-cells to ER stress and apoptosis. Investigation of Anks4b knock-out mice will improve our understanding of the role of this molecule in ER stress. Anks4b does not possess the canonical ER localization signal (35), so the molecular mechanism by which Anks4b binds to GRP78 and regulates ER stress warrants further investigation.

HNF4α plays an important role in a number of metabolic pathways, including those for gluconeogenesis, ureagenesis, fatty acid metabolism, and drug metabolism (36–38). Our finding that Anks4b is a target of HNF4α uncovers a new role for this transcription factor in regulating β-cell susceptibility to ER stress. ER stress is associated with β-cell apoptosis in common type 2 diabetes (39). Because reduced expression of Anks4b was associated with a decrease, rather than an increase, of ER stress and apoptosis, the significance of Anks4b in relation to the occurrence of MODY is unclear. However, recent genetic studies have shown that HNF4α has dual opposing roles in the β-cell during different periods of life. Although HNF4α deficiency results in diabetes in young adults (6), the same genetic defect occasionally causes hyperinsulinemic hypoglycemia at birth (40, 41). Further studies will need to address whether reduced Anks4b expression is responsible for the hypersecretion of β-cells early in life.

In conclusion, we identified Anks4b as a novel molecule that controls the susceptibility to ER stress-induced apoptosis. The ER is critical for the normal functioning of pancreatic β-cells, and ER stress-associated apoptosis is often a contributory factor to β-cell death in type 2 diabetes (39). Therefore, Anks4b may be a potential target for the treatment of diabetes associated with ER stress.

Acknowledgments—We thank Prof. J. Miyazaki (Osaka University) for the gift of MIN6 cells, Prof. T. Kitamura (Tokyo University) for providing the Plat-E cells and pMXs vector, and Dr. T. Tanaka (Tokyo University) for providing pcDNA3-HNF4α7 plasmid.

REFERENCES

1. Sladek, F. M., Zhong, W. M., Lai, E., and Darnell, J. E. (1990) Liver-enriched transcription factor HNF-4 is a novel member of the steroid hormone receptor superfamily. *Genes Dev.* **4,** 2353–2365
2. Nammo, T., Yamagata, K., Tanaka, T., Kodama, T., Sladek, F. M., Fukui, K., Katsube, F., Sato, Y., Miyagawa, J., and Shimomura, I. (2008) Expression of HNF-4α (MODY1), HNF-1β (MODY5), and HNF-1α (MODY3) proteins in the developing mouse pancreas. *Gene Expr. Patterns* **8,** 96–106
3. Hadzopoulou-Cladaras, M., Kistanova, E., Evagelopoulou, C., Zeng, S., Cladaras, C., and Ladias, J. A (1997) Functional domains of the nuclear receptor hepatocyte nuclear factor 4. *J. Biol. Chem.* **272,** 539–550
4. Ihara, A., Yamagata, K., Nammo, T., Miura, A., Yuan, M., Tanaka, T., Sladek, F. M., Matsuzawa, Y., Miyagawa, J., and Shimomura, I. (2005) Functional characterization of the HNF4α isoform (HNF4α8) expressed in pancreatic β-cells. *Biochem. Biophys. Res. Commun.* **329,** 984–990
5. Bell, G. I., and Polonsky, K. S. (2001) Diabetes mellitus and genetically programmed defects in β-cell function. *Nature* **414,** 788–791
6. Yamagata, K., Furuta, H., Oda, N., Kaisaki, P. J., Menzel, S., Cox, N. J., Fajans, S. S., Signorini, S., Stoffel, M., and Bell, G. I. (1996) Mutations in the hepatocyte nuclear factor-4α gene in maturity-onset diabetes of the young (MODY1) *Nature* **384,** 458–460
7. Miura, A., Yamagata, K., Kakei, M., Hatakeyama, H., Takahashi, N., Fukui, K., Nammo, T., Yoneda, K., Inoue, Y., Sladek, F. M., Magnuson, M. A., Kasai, H., Miyagawa, J., Gonzalez, F. J., and Shimomura, I. (2006) Hepatocyte nuclear factor-4α is essential for glucose-stimulated insulin secretion by pancreatic β-cells. *J. Biol. Chem.* **281,** 5246–5257
8. Gupta, R. K., Vatamaniuk, M. Z., Lee, C. S., Flaschen, R. C., Fulmer, J. T., Matschinsky, F. M., Duncan, S. A., and Kaestner, K. H. (2005) The MODY1 gene HNF-4α regulates selected genes involved in insulin secretion. *J. Clin. Invest.* **115,** 1006–1015
9. Hayhurst, G. P., Lee, Y. H., Lambert, G., Ward, J. M., and Gonzalez, F. J. (2001) Hepatocyte nuclear factor 4α (nuclear receptor 2A1) is essential for maintenance of hepatic gene expression and lipid homeostasis. *Mol. Cell Biol.* **21,** 1393–1403
10. Rhee, J., Inoue, Y., Yoon, J. C., Puigserver, P., Fan, M., Gonzalez, F. J., and Spiegelman, B. M. (2003) Regulation of hepatic fasting response by PPARγ coactivator-1α (PGC-1): requirement for hepatocyte nuclear factor 4α in gluconeogenesis. *Proc. Natl. Acad. Sci. U.S.A.* **100,** 4012–4017

11. Wang, H., Maechler, P., Antinozzi, P. A., Hagenfeldt, K. A., and Wollheim, C. B. (2000) Hepatocyte nuclear factor 4α regulates the expression of pancreatic β-cell genes implicated in glucose metabolism and nutrient-induced insulin secretion. *J. Biol. Chem.* **275,** 35953–35959
12. Sato, Y., Endo, H., Okuyama, H., Takeda, T., Iwahashi, H., Imagawa, A., Yamagata, K., Shimomura, I., and Inoue, M. (2011) Cellular hypoxia of pancreatic β-cells due to high levels of oxygen consumption for insulin secretion in vitro. *J. Biol. Chem.* **286,** 12524–12532
13. Miyazaki, J., Araki, K., Yamato, E., Ikegami, H., Asano, T., Shibasaki, Y., Oka, Y., and Yamamura, K. (1990) Establishment of a pancreatic β-cell line that retains glucose-inducible insulin secretion: special reference to expression of glucose transporter isoforms. *Endocrinology* **127,** 126–132
14. Yang, Q., Yamagata, K., Yamamoto, K., Cao, Y., Miyagawa, J., Fukamizu, A., Hanafusa, T., and Matsuzawa, Y. (2000) R127W-HNF-4α is a loss-of-function mutation but not a rare polymorphism and causes type II diabetes in a Japanese family with MODY1. *Diabetologia* **43,** 520–524
15. Yamagata, K., Yang, Q., Yamamoto, K., Iwahashi, H., Miyagawa, J., Okita, K., Yoshiuchi, I., Miyazaki, J., Noguchi, T., Nakajima, H., Namba, M., Hanafusa, T., and Matsuzawa, Y. (1998) Mutation P291fsinsC in the transcription factor hepatocyte nuclear factor-1α is dominant negative. *Diabetes* **47,** 1231–1235
16. Dignam, J. D., Lebovitz, R. M., and Roeder, R. G. (1983) Accurate transcription initiation by RNA polymerase II in a soluble extract from isolated mammalian nuclei. *Nucleic Acids Res.* **11,** 1475–1489
17. Shevchenko, A., Wilm, M., Vorm, O., and Mann, M. (1996) Mass spectrometric sequencing of proteins silver-stained polyacrylamide gels. *Anal. Chem.* **68,** 850–858
18. Kitamura, T., Koshino, Y., Shibata, F., Oki, T., Nakajima, H., Nosaka, T., and Kumagai, H. (2003) Retrovirus-mediated gene transfer and expression cloning: powerful tools in functional genomics. *Exp. Hematol.* **31,** 1007–1014
19. Gupta, R. K., Gao, N., Gorski, R. K., White, P., Hardy, O. T., Rafiq, K., Brestelli, J. E., Chen, G., Stoeckert, C. J., Jr., and Kaestner, K. H. (2007) Expansion of adult β-cell mass in response to increased metabolic demand is dependent on HNF-4α. *Genes Dev.* **21,** 756–769
20. Pontoglio, M., Barra, J., Hadchouel, M., Doyen, A., Kress, C., Bach, J. P., Babinet, C., and Yaniv, M. (1996) Hepatocyte nuclear factor 1 inactivation results in hepatic dysfunction, phenylketonuria, and renal Fanconi syndrome. *Cell* **84,** 575–585
21. Yamagata, K., Oda, N., Kaisaki, P. J., Menzel, S., Furuta, H., Vaxillaire, M., Southam, L., Cox, R. D., Lathrop, G. M., Boriraj, V. V., Chen, X., Cox, N. J., Oda, Y., Yano, H., Le Beau, M. M., Yamada, S., Nishigori, H., Takeda, J., Fajans, S. S., Hattersley, A. T., Iwasaki, N., Hansen, T., Pedersen, O., Polonsky, K. S., and Bell, G. I. (1996) Mutations in the hepatocyte nuclear factor-1α gene in maturity-onset diabetes of the young (MODY3) *Nature* **384,** 455–458
22. Servitja, J. M., Pignatelli, M., Maestro, M. A., Cardalda, C., Boj, S. F., Lozano, J., Blanco, E., Lafuente, A., McCarthy, M. I., Sumoy, L., Guigó, R., and Ferrer, J. (2009) Hnf1α (MODY3) controls tissue-specific transcriptional programs and exerts opposed effects on cell growth in pancreatic islets and liver. *Mol. Cell Biol.* **29,** 2945–2959
23. Ozeki, T., Takahashi, Y., Kume, T., Nakayama, K., Yokoi, T., Nunoya, K., Hara, A., and Kamataki, T. (2001) Cooperative regulation of the transcription of human dihydrodiol dehydrogenase (*DD)4*/aldo-keto reductase (*AKR)1C4* gene by hepatocyte nuclear factor (HNF)-4α/γ and HNF-1α. *Biochem. J.* **355,** 537–544
24. Eeckhoute, J., Formstecher, P., and Laine, B. (2004) Hepatocyte nuclear factor 4α enhances the hepatocyte nuclear factor 1α-mediated activation of transcription. *Nucleic Acids Res.* **32,** 2586–2593
25. Johnston, A. M., Naselli, G., Niwa, H., Brodnicki, T., Harrison, L. C., and Góñez, L. J. (2004) Harp (harmonin-interacting, ankyrin repeat-containing protein), a novel protein that interacts with harmonin in epithelial tissues. *Genes Cells* **9,** 967–982
26. Zhang, L. H., and Zhang, X. (2010) Roles of GRP78 in physiology and cancer. *Journal of cellular biochemistry* **110,** 1299–1305
27. Wang, M., Wey, S., Zhang, Y., Ye, R., and Lee, A. S. (2009) Role of the unfolded protein response regulator GRP78/BiP in development, cancer, and neurological disorders. *Antioxid. Redox Signal.* **11,** 2307–2316
28. Morris, J. A., Dorner, A. J., Edwards, C. A., Hendershot, L. M., and Kaufman, R. J. (1997) Immunoglobulin-binding protein (BiP) function is required to protect cells from endoplasmic reticulum stress but is not required for the secretion of selective proteins. *J. Biol. Chem.* **272,** 4327–4334
29. Wang, X. Z., Lawson, B., Brewer, J. W., Zinszner, H., Sanjay, A., Mi, L. J., Boorstein, R., Kreibich, G., Hendershot, L. M., and Ron, D. (1996) Signals from the stressed endoplasmic reticulum induce C/EBP-homologous protein (CHOP/GADD153). *Mol. Cell Biol.* **16,** 4273–4280
30. Treiman, M., Caspersen, C., and Christensen, S. B. (1998) A tool coming of age: thapsigargin as an inhibitor of sarco-endoplasmic reticulum Ca^{2+}-ATPases. *Trends Pharmacol. Sci.* **19,** 131–135
31. Lai, E., Teodoro, T., and Volchuk, A. (2007) Endoplasmic reticulum stress: signaling the unfolded protein response. *Physiology* **22,** 193–201
32. Fukui, K., Yang, Q., Cao, Y., Takahashi, N., Hatakeyama, H., Wang, H., Wada, J., Zhang, Y., Marselli, L., Nammo, T., Yoneda, K., Onishi, M., Higashiyama, S., Matsuzawa, Y., Gonzalez, F. J., Weir, G. C., Kasai, H., Shimomura, I., Miyagawa, J., Wollheim, C. B., and Yamagata, K. (2005) The HNF-1 target collectrin controls insulin exocytosis by SNARE complex formation. *Cell Metab.* **2,** 373–384
33. Akpinar, P., Kuwajima, S., Krützfeldt, J., and Stoffel, M. (2005) Tmem27: a cleaved and shed plasma membrane protein that stimulates pancreatic β-cell proliferation. *Cell Metab.* **2,** 385–397
34. Boj, S. F., Petrov, D., and Ferrer, J. (2010) Epistasis of transcriptomes reveals synergism between transcriptional activators Hnf1α and Hnf4α. *PLoS genet.* **6,** e1000970
35. Pagny, S., Lerouge, P., Faye, L., and Gomord, V. (1999) Signals and mechanisms for protein retention in the endoplasmic reticulum. *J. Exp. Bot.* **50,** 157–164
36. Sladek, F. M., and Seidel, S. D. (2001) in *Nuclear Receptors and Genetic Diseases* (Burris, T. P., and McCabe, E., eds) pp. 309–361, Academic Press, London, UK
37. Gonzalez, F. J. (2008) Regulation of hepatocyte nuclear factor 4α-mediated transcription. *Drug Metab. Pharmacokinet.* **23,** 2–7
38. Bolotin, E., Liao, H., Ta, T. C., Yang, C., Hwang-Verslues, W., Evans, J. R., Jiang, T., and Sladek, F. M. (2010) Integrated approach for the identification of human hepatocyte nuclear factor 4α target genes using protein binding microarrays. *Hepatology* **51,** 642–653
39. Marchetti, P., Bugliani, M., Lupi, R., Marselli, L., Masini, M., Boggi, U., Filipponi, F., Weir, G. C., Eizirik, D. L., and Cnop, M. (2007) The endoplasmic reticulum in pancreatic β-cells of type 2 diabetes patients. *Diabetologia* **50,** 2486–2494
40. Pearson, E. R., Boj, S. F., Steele, A. M., Barrett, T., Stals, K., Shield, J. P., Ellard, S., Ferrer, J., and Hattersley, A. T. (2007) Macrosomia and hyperinsulinemic hypoglycemia in patients with heterozygous mutations in the HNF4A gene. *PLoS Med.* **4,** e118
41. Kapoor, R. R., Locke, J., Colclough, K., Wales, J., Conn, J. J., Hattersley, A. T., Ellard, S., and Hussain, K. (2008) Persistent hyperinsulinemic hypoglycemia and maturity-onset diabetes of the young due to heterozygous HNF4A mutations. *Diabetes* **57,** 1659–1663

Biochemical and Biophysical Research Communications 425 (2012) 619–624

Contents lists available at SciVerse ScienceDirect

Biochemical and Biophysical Research Communications

journal homepage: www.elsevier.com/locate/ybbrc

Identification of hepatocyte growth factor activator (Hgfac) gene as a target of HNF1α in mouse β-cells

Tsuyoshi Ohki [a,b], Yoshifumi Sato [a], Tatsuya Yoshizawa [a], Ken-ichi Yamamura [c], Kentaro Yamada [b], Kazuya Yamagata [a,*]

[a] Department of Medical Biochemistry, Faculty of Life Sciences, Kumamoto University, Kumamoto, Japan
[b] Division of Endocrinology and Metabolism, Kurume University School of Medicine, Kurume, Japan
[c] Division of Developmental Genetics, Center for Animal Resources and Development, Institute of Resource Development and Analysis, Kumamoto University, Kumamoto, Japan

ARTICLE INFO

Article history:
Received 24 July 2012
Available online 1 August 2012

Keywords:
Diabetes mellitus
HNF1α
Transcription factor
Pancreatic β-cell
HGF

ABSTRACT

HNF1α is a transcription factor that is expressed in pancreatic β-cells and mutations of the HNF1α gene cause a form of monogenic diabetes. To understand the role of HNF1α in pancreatic β-cells, we established the MIN6 β-cell line that stably expressed HNF1α-specific shRNA. Expression of the gene encoding hepatocyte growth factor (HGF) activator (Hgfac), a serine protease that efficiently activates HGF, was decreased in HNF1α KD-MIN6 cells. Down-regulation of *Hgfac* expression was also found in the islets of HNF1α (+/−) mice. Reporter gene analysis and the chromatin immunoprecipitation assay indicated that HNF1α directly regulates the expression of *Hgfac* in β-cells. It has been reported that HGF has an important influence on β-cell mass and β-cell function. Thus, HNF1α might regulate β-cell mass or function at least partly by modulating Hgfac expression.

1. Introduction

HNF1α is a transcription factor that belongs to a subclass of the homeodomain family, and it is expressed in the liver, pancreas, kidney, and intestine [1,2]. HNF1α has an N-terminal dimerization domain, a DNA-binding domain with POU-like and homeodomain-like motifs, and a C-terminal transactivation domain [3]. We previously reported that heterozygous mutations of the HNF1α gene cause a form of monogenic diabetes known as maturity-onset diabetes of the young type 3 (MODY3) [4]. Clinical studies have shown that the primary cause of MODY3 is impairment of insulin secretion in response to a glucose load [5]. Mutant mice with loss of HNF1α function also develop diabetes due to impaired insulin secretion [6,7], indicating an important role of HNF1α in pancreatic β-cells. Interestingly, these mutant mice exhibit progressive reduction of β-cell numbers, suggesting that some target genes of HNF1α are also required for the maintenance of a normal β-cell mass.

To better understand the role of HNF1α in pancreatic β-cells and in the molecular mechanisms of MODY3, identification of the full spectrum of genes regulated by this factor in β-cells is necessary. Previous studies have demonstrated that *Slc2a2* (encoding glucose transporter 2 (GLUT2)), *Pklr* (encoding liver pyruvate kinase), *Tmem27* (encoding collectrin), *Hnf4a* (encoding HNF4α), and *Foxa3* (encoding HNF3γ) are direct targets of HNF1α in β-cells [8–12]. Genome-wide expression profiling has also been performed to identify additional targets of HNF1α using pancreatic islets obtained from control and HNF1α (−/−) knockout (KO) mice [13]. Although this approach revealed that expression of 5.6% of all genes was down-regulated in HNF1α KO islets, these changes might have been secondary to the onset of hyperglycemia or other effects of the diabetic state in HNF1α KO mice.

To identify the direct target genes of HNF1α in β-cells by another approach, we established the MIN6 β-cell line that stably expressed HNF1α-specific shRNA (HNF1α KD-MIN6 cells) and then compared the gene expression profile between control MIN6 cells and HNF1α KD-MIN6 cells. As a result, we demonstrated the down-regulation of several genes, including *Slc2a2*, *Tmeme27*, and *Hnf4a*, in HNF1α KD-MIN6 cells. We also found that expression of the gene encoding hepatocyte growth factor (HGF) activator (Hgfac), a serine protease that efficiently activates HGF [14], was decreased in HNF1α KD-MIN6 cells. Down-regulation of *Hgfac* expression was also found in the islets of HNF1α (+/−) mice. Reporter gene analysis and the chromatin immunoprecipitation assay confirmed that HNF1α directly regulates the expression of *Hgfac* in β-cells.

* Corresponding author. Address: Department of Medical Biochemistry, Faculty of Life Sciences, Kumamoto University, 1-1-1 Honjo, Kumamoto, Kumamoto 860-8556, Japan. Fax: +81 96 364 6940.
E-mail address: k-yamaga@kumamoto-u.ac.jp (K. Yamagata).

0006-291X/$ - see front matter © 2012 Elsevier Inc. All rights reserved.
http://dx.doi.org/10.1016/j.bbrc.2012.07.134

2. Material and methods

2.1. Cell culture

The MIN6 pancreatic β-cell line was maintained in Dulbecco's modified Eagles' medium (DMEM) (25 mM glucose) containing 10% (v/v) fetal bovine serum, 50 μM β-mercaptoethanol (β-ME), 50 U/ml penicillin, and 50 μg/ml streptomycin at 37 °C under 5% CO_2 [15]. Hela cells and Plat-E retrovirus packaging cells [16] were maintained in DMEM containing 10% (v/v) fetal bovine serum.

2.2. Retroviral infection

A specific shRNA sequence for mouse HNF1α (5′-CGAAGATGGTCAAGTCGTA-3′) was designed using the Clontech RNAi target sequence (http://bioinfo.clontech.com/). Oligonucleotides encoding shRNA were synthesized and cloned into the pSIREN-RetroQ retroviral shRNA expression vector (Clontech/Takara, Japan). Then the pSIREN-RetroQ-HNF1α vector and the negative control pSIREN-RetroQ vector were transfected into Plat-E cells using FuGENE6 (Roch, Germany). MIN6 cells were infected with either retrovirus and then selected by incubation with puromycin (5 μg/ml) to generate MIN6 cells stably expressing HNF1α shRNA (HNF1α KD-MIN6 cells) or negative control shRNA (control MIN6 cells), as described previously [17].

2.3. Quantitative RT-PCR

Total RNA was extracted by using Sepasol RNA I super reagent (Nacalai Tesque, Japan) or an RNeasy micro kit (Qiagen, CA). Quantitative real-time PCR was performed with SYBR Premix Ex Taq II (RR820A, TaKaRa) in an ABI 7300 thermal cycler (Applied Biosystems, CA). The specific primers were as follows: *Hnf1α* (5′-AAGAGCCCACAGGCGATGAG-3′ and 5′-TGGATGCACTCCGCCCTATT-3′), *Hgfac* (5′-GCACCTGCCACCTGATTGTG-3′ and 5′-GCCACGCCTCG GTACTCTGT-3′), *Slc2a2* (5′-CGTCCTACGGCTCTGGCACT-3′ and 5′-CACCCCAGCGAAGAGGAAGA-3′), *Tmem27* (5′-ATTCGGTGTGATATT TTGCATTGT-3′ and 5′-TCCAGGTGGTCCTTTGTTGTT-3′), and TATA-binding protein (*Tbp*) (5′-CCCCTTGTACCCTTCACCAAT-3′ and 5′-GAAGCTGCGGTACAATTCCAG-3′). Relative expression of each gene was normalized for that of *Tbp*.

2.4. Western blotting

Cells were lysed in RIPA buffer (50 mM Tris–HCl (pH 8.0), 150 mM NaCl, 0.1% SDS, 1% NP-40, 5 mM EDTA, 0.5% sodium deoxycholate), and 1/100 (v/v) protease inhibitor cocktail (Nacalai Tesque). Total protein was separated by SDS polyacrylamide gel electrophoresis and transferred to a polyvinylidene fluoride (PVDF) membrane (ImmobilonP; Millipore, MA), which was probed with the primary antibodies. After incubation with the secondary antibodies, proteins were visualized using Chemi-Lumi One Super (Nacalai Tesque) and a LAS-1000 imaging system (Fuji Film, Japan). The primary antibodies used in this study were anti-HNF1α (1:1000) (610902; Becton, Dickinson and Company, NJ) and anti-β-actin (1:5000) (A5441; Sigma–Aldrich, MO).

2.5. Insulin secretion

After reaching 80% confluence, MIN6 cells were plated in 24-well plates at a density of 3×10^5 cells per well. After culture for 72 h, cells were preincubated at 37 °C for 60 min in Hepes–Krebs buffer (118.4 mM NaCl, 4.7 mM KCl, 1.2 mM KH_2PO_4, 2.4 mM $CaCl_2$, 1.2 mM $MgSO_4$, 20 mM $NaHCO_3$, 2.2 mM glucose, and 10 mM Hepes) containing 0.5% (w/v) bovine serum albumin (BSA) [17]. Then the cells were incubated for 60 min in Hepes–Krebs buffer containing 22 mM glucose and insulin production was measured by using a mouse insulin ELISA kit (AKRIN-011T; Shibayagi, Japan).

2.6. Microarray analysis

Total RNA was extracted from control MIN6 cells and HNF1α KD-MIN6 cells using a miRCURY RNA isolation kit (Exiqon, Denmark) according to the manufacturer's instructions. The quality of the RNA was checked by gel electrophoresis and analysis with an Agilent 2100 Bioanalyzer (Agilent Technologies, CA). DNA microarray analysis was performed by the Toray Custom Analysis Service using the 3D-Gene™ DNA chip (Mouse Oligo chip 24K).

2.7. Isolation of pancreatic islets

HNF1α knockout mice were generated that lacked exon 1, which contains the translation start codon [K. Yamamura, and K. Yamagata, unpublished data]. HNF1α (+/−) mice showed normal glucose tolerance, as reported previously [6, and our unpublished data]. Mice were maintained with a 12 h light–12 h dark cycle and were allowed free access to food and water. These experiments were conducted according to the guidelines of the Institutional Animal Committee of Kumamoto University. Islets were isolated from the harvested pancreata of 20-week-old male HNF1α (+/−) mice ($n = 4$) and control HNF1α (+/+) littermates ($n = 4$) by collagenase digestion, as described previously [7].

2.8. Transient transfection and luciferase reporter assay

A 135 bp fragment of the mouse Hgfac gene promoter containing the putative HNF1α-binding site (−135 to −1 relative to the translation start codon when A is numbered as +1) was amplified by PCR using the primers 5′-GCTAGCGGCTGTGGAGGAGCCTAACAGGAT-3′ (underlined nucleotides indicate the cloned NheI site) and 5′-AAGCTTGGCTCCTCCTGAGCTGGCGTGAGG-3′ (underlined nucleotides indicate the cloned HindIII site), and then was subcloned into the pGL3 basic reporter (Promega, WI) to generate pGL3-Hgfac. The HNF1α-binding site was altered to 5′-GGTCGGCCCTTATCA-3′ by PCR-based mutagenesis. The pcDNA3.1-wild-type (WT)-HNF1α and pcDNA3.1-P291fsinsC-HNF1α expression plasmids have been described previously [8]. Hela cells (1.5×10^5 cells/well) or MIN6 cells (3×10^5 cells/well) were seeded into 12-well plates at 18 h before transient transfection was performed using X-treme GENE (Roche) according to the manufacturer's instructions. At 48 h after transfection, luciferase activity was measured by using a Dual-Luciferase Reporter assay system (Promega).

2.9. Chromatin immunoprecipitation (ChIP) assay

MIN6 cells were cross-linked with 1% formaldehyde for 10 min at room temperature. Then the ChIP assay was performed as described previously [17] using an anti-HNF1 antibody (sc-8986, Santa Cruz Biotechnology, CA). Immunoprecipitated DNA was amplified by real-time PCR with specific primers for the promoter region of *Hgfac* containing the HNF1α-binding motif (5′-GGCTGTG GAGGAGCCTAACAGGAT-3′ and 5′-GGCTCCTCCTGAGCTGGCGT-GAGG-3′) (P1), as well as primers for the 10 kb upstream region from the *Hgfac* translation start codon (5′-GGGCTGGGGT GC TTCGGGTA-3′ and 5′-GACCCTCCAGCGGATGGC TCA-3′) (P2), the 5.3 kb downstream region from the *Hgfac* translation start (5′-GCTGTGCTGTCCGCTCCCAG-3′ and 5′-CATGTGGCCCCAGCCTGCAA-3′) (P3), and the promoter region of *Tbp* (5′-ATCAGATGTGCGT-CAGGCGTT-3′ and 5′-TGCGGAGAAAATGACGCGA-3′) (P4). All PCR

reactions were done by using SYBR Premix Ex Taq II (TaKaRa) in an ABI 7300 thermal cycler (Applied Biosystems).

2.10. Statistical analysis

The significance of differences was assessed with the unpaired *t*-test, and $p < 0.05$ was considered to indicate statistical significance.

3. Results

3.1. Establishment of HNF1α KD-MIN6 cells and microarray analysis

In order to identify novel target genes for HNF1α in pancreatic β-cells, we established MIN6 β-cells that stably expressed HNF1α-specific shRNA (HNF1α KD-MIN6) by retroviral infection. Suppression of endogenous HNF1α expression by shRNA was confirmed at both the mRNA level (39.8% of control, $p = 0.019$) and the protein level (30.6% of control, $p = 0.007$) (Fig. 1A and B). *Slc2a2* and *Tmem27* are direct targets of HNF1α in β-cells [10,11], and expression of both these genes was significantly decreased in HNF1α KD-MIN6 cells (Fig. 1C). Loss of the function of HNF1α leads to impairment of glucose-stimulated insulin secretion by pancreatic β-cells [6,7]. Therefore, we examined insulin secretion by HNF1α KD-MIN6 cells and control MIN6 cells. Insulin secretion by HNF1α KD-MIN6 cells subjected to stimulation with 22 mM glucose was significantly decreased ($p < 0.001$) to 39.2% of that for control cells (Fig. 1D). Suppression of HNF1α expression also reduced insulin secretion by HNF1α KD-MIN6 cells in response to a low glucose concentration (decreased by 41.4%, $p < 0.001$). These results indicate that HNF1α KD-MIN6 cells can be used as a novel cellular model of MODY3.

In order to identify novel target genes of HNF1α in pancreatic β-cells, DNA microarray analysis was performed using control cells and HNF1α KD-MIN6 cells. Microarray analysis identified the down-regulation of 53 genes (0.22% of all expressed genes), which was defined as a signal log ratio $\leqslant -1.5$, in HNF1α KD-MIN6 cells and up-regulation of 38 genes (0.15% of all expressed genes), which was defined as a signal log ratio $\geqslant 2$ (Table 1 and Supplementary Table 1). Several known targets of HNF1α (*Slc2a2*, *Tmem27*, and *Hnf4α*) were found in the group of down-regulated genes.

3.2. Hgfac expression in β-cells is regulated by HNF1α

Microarray analysis revealed that expression of the gene encoding hepatocyte growth factor activator (HGFA) was reduced to 25.2% of the control level in HNF1α KD-MIN6 cells (Table 1). Down-regulation of *Hgfac* expression in HNF1α KD-MIN6 cells to 18.7% of the control level ($p < 0.001$) was confirmed by quantitative RT-PCR (Fig. 2A). HNF1α (+/−) mice were reported to be useful for investigating HNF1α-dependent transcription in pancreatic islets [18]. As shown in Fig. 2B, Hgfac mRNA expression was significantly decreased in the islets of HNF1α (+/−) mice to 45.8% of the control level ($p < 0.001$), indicating that *Hgfac* gene transcription is regulated by HNF1α *in vivo* as well as *in vitro*.

Screening of the promoter region of the mouse *Hgfac* gene by using a genomic databank revealed an HNF1α-binding site (nucleotides −83 to −97 relative to the translation start codon when *A* is designated as +1), and this binding site was also confirmed to exist in the human HGFAC gene (Fig. 2C). We cloned a 135 bp fragment

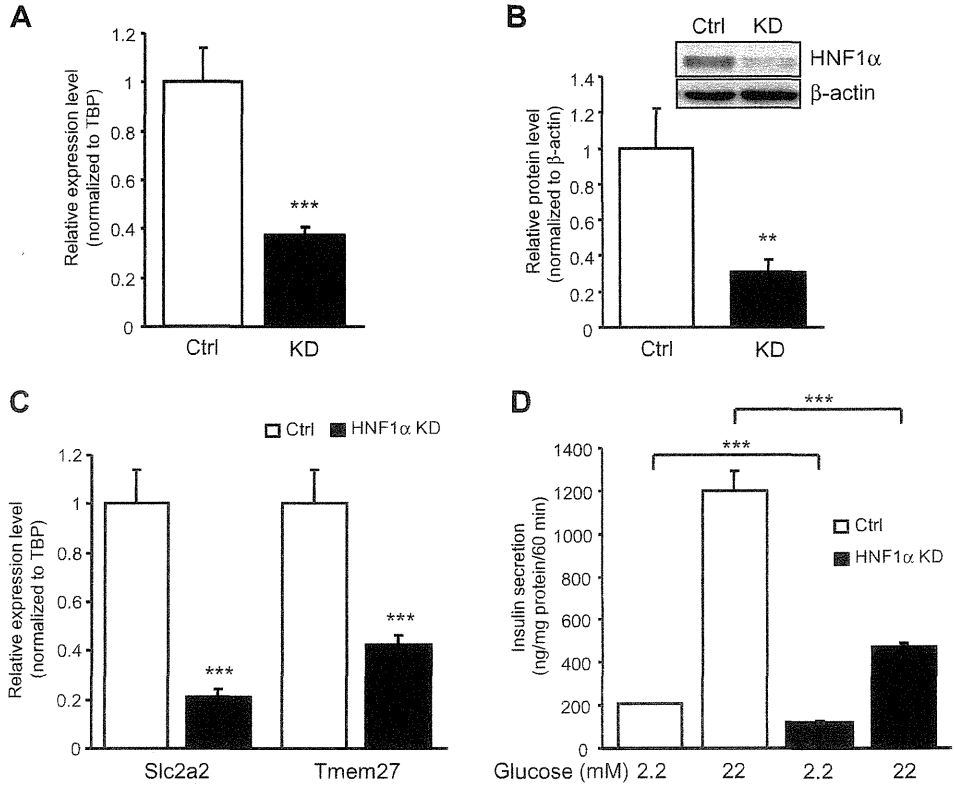

Fig. 1. Gene expression and insulin secretion by HNF1α KD-MIN6 cells. (A) Expression of HNF1α mRNA by control cells (Ctrl) ($n = 3$) and HNF1α KD-MIN6 cells (KD) ($n = 3$). Expression is normalized for that of Tbp. (B) HNF1α protein expression in HNF1α KD-MIN6 cells evaluated by Western blotting ($n = 3$). β-actin was used as the loading control. (C) Expression of Slc2a2 and Tmem27 mRNA was significantly decreased in HNF1α KD-MIN6 cells ($n = 3$). (D) Insulin secretion after exposure to glucose was decreased in HNF1α KD-MIN6 cells ($n = 4$). Data are the mean ± SD ($^{**}p < 0.01$, $^{***}p < 0.001$).

Table 1
Gene list of the down-regulated genes in HNF1α KD-MIN6 cells.

Gene symbol	Gene title	Log ratio	RefSeq transcript ID
Gc	Group specific component	−3.76	NM_008096
Ugt1a6a	UDP glucuronosyltransferase 1 family, polypeptide A7C	−3.68	NM_145079
Slc2a2	Solute carrier family 2 (facilitated glucose transporter), member 2	−3.61	NM_031197
Crp	C-reactive protein, pentraxin-related	−3.48	NM_007768
Ttr	Transthyretin	−3.23	NM_013697
Tmed6	Transmembrane emp24 protein transport domain containing 6	−3.02	NM_025458
Serpina1c	Serine (or cysteine) peptidase inhibitor, clade A, member 1a	−2.90	NM_009245
Iyd	Iodotyrosine deiodinase	−2.80	NM_027391
Slc40a1	Solute carrier family 40 (iron-regulated transporter), member 1	−2.70	NM_016917
Ang1	Angiogenin, ribonuclease A family, member 1	−2.70	NM_007447
Spon2	Spondin 2, extracellular matrix protein	−2.64	NM_133903
Rnase4	Ribonuclease, RNase A family 4	−2.62	NM_021472
Golt1a	Golgi transport 1 homolog A (S. cerevisiae)	−2.53	NM_026680
Serpina1c	Serine (or cysteine) peptidase inhibitor, clade A, member 1a	−2.50	NM_009243
Serpina1d	Serine (or cysteine) peptidase inhibitor, clade A, member 1d	−2.44	NM_009246
Serpina1e	Serine (or cysteine) peptidase inhibitor, clade A, member 1e	−2.33	NM_009247
Guca1a	Guanylate cyclase activator 1a (retina)	−2.29	NM_008189
Nmbr	Neuromedin B receptor	−2.29	NM_008703
Tmem27	Transmembrane protein 27	−2.26	NM_020626
Ang4	Angiogenin, ribonuclease A family, member 4	−2.24	NM_177544
Ang5	Angiogenin, ribonuclease A family, member 5	−2.21	NM_007448
Dpp4	Dipeptidylpeptidase 4	−2.20	NM_010074
Ldha	Lactate dehydrogenase A	−2.11	NM_010699
St6gal1	Beta galactoside alpha 2,6 sialyltransferase 1	−2.05	NM_145933
Hgfac	Hepatocyte growth factor activator	−1.99	NM_019447
Pcsk9	Proprotein convertase subtilisin/kexin type 9	−1.98	NM_153565
Ang5	Angiogenin, ribonuclease A family, member 5	−1.97	NM_007448
Abcg2	ATP-binding cassette, sub-family G (WHITE), member 2	−1.96	NM_011920
Ins1	Insulin I	−1.92	NM_008386
Kif12	Kinesin family member 12	−1.89	NM_010616
Ppp1r1a	Protein phosphatase 1, regulatory (inhibitor) subunit 1A	−1.87	NM_021391
Itga6	Integrin alpha 6	−1.84	NM_008397
Myo15b	Myosin XVB	−1.84	XM_203357
Il20rb	Interleukin 20 receptor beta	−1.83	XM_358706
Degs2	Degenerative spermatocyte homolog 2 (Drosophila), lipid desaturase	−1.81	NM_027299
Tff3	Trefoil factor 3, intestinal	−1.75	NM_011575
Cpn1	Carboxypeptidase N, polypeptide 1	−1.71	NM_030703
Cbs	Cystathionine beta-synthase	−1.71	NM_144855
Insl5	Insulin-like 5	−1.70	NM_011831
Slc16a3	Solute carrier family 16 (monocarboxylic acid transporters), member 3	−1.70	NM_030696
Mbl2	Mannose binding lectin (protein C)	−1.68	NM_010776
Tm4sf4	Transmembrane 4 superfamily member 4	−1.67	NM_145539
Dact2	Dapper homolog 2, antagonist of beta-catenin (xenopus)	−1.63	NM_172826
Dscr1l1	Down syndrome critical region gene 1-like 1	−1.63	NM_030598
Anks4b	Ankyrin repeat and sterile alpha motif domain containing 4B	−1.61	NM_028085
Cacna1 h	Calcium channel, voltage-dependent, T type, alpha 1H subunit	−1.60	NM_021415
Il6ra	Interleukin 6 receptor, alpha	−1.59	NM_010559
Hnf4a	Hepatic nuclear factor 4, alpha	−1.59	NM_008261
Defb1	Defensin beta 1	−1.58	NM_007843
Sgk2	Serum/glucocorticoid regulated kinase 2	−1.56	NM_013731
Sct	Secretin	−1.52	NM_011328
Lgals2	Lectin, galactose-binding, soluble 2	−1.52	NM_025622
Nek6	NIMA (never in mitosis gene a)-related expressed kinase 6	−1.51	NM_021606

of the promoter region upstream of a luciferase reporter gene, and co-expressed it with the HNF1α expression vector in HeLa cells. We found that induction of HNF1α increased *Hgfac* promoter activity to 23.6 times the control level ($p < 0.001$) (Fig. 2D). HNF1α also activated the reporter gene by 3.1-fold ($p < 0.001$) in MIN6 cells, while dominant negative P291fsinsC-HNF1α (a frameshift mutation in the transactivation domain) [8] decreased reporter gene activity to 41.0% of the control level ($p < 0.001$) (Fig. 2E). Mutation of the putative HNF1α-binding site in the reporter gene significantly reduced transcriptional activation by HNF1α (87.3% decrease, $p < 0.001$) (Fig. 2F).

In order to investigate binding of HNF1α to the Hgfac promoter, the chromatin immunoprecipitation (ChIP) assay was performed. Cross-linked chromatin was precipitated with HNF1 antibody, after which the precipitated DNA was analyzed by PCR using primer sets that amplified the promoter region of *Hgfac* containing the putative HNF1α-binding site (P1), the 10 kb upstream region from P1 (P2), the 5.3 kb downstream region from P1 (exon 12) (P3), and the promoter region of *Tbp* (P4). As shown in Fig. 2G, specific binding of HNF1α to the promoter region (P1) was identified in MIN6 cells. These findings indicated that the *Hgfac* gene is directly regulated by HNF1α.

4. Discussion

HGF was originally identified as a potent mitogen for hepatocytes [19], but subsequent studies have shown that it has mitogenic and prosurvival effects on various cells including β-cells. Transgenic overexpression of HGF in pancreatic β-cells increases β-cell replication, mass, and function [20]. Loss of HGF signaling in β-cells during gestation leads to decreased replication and a

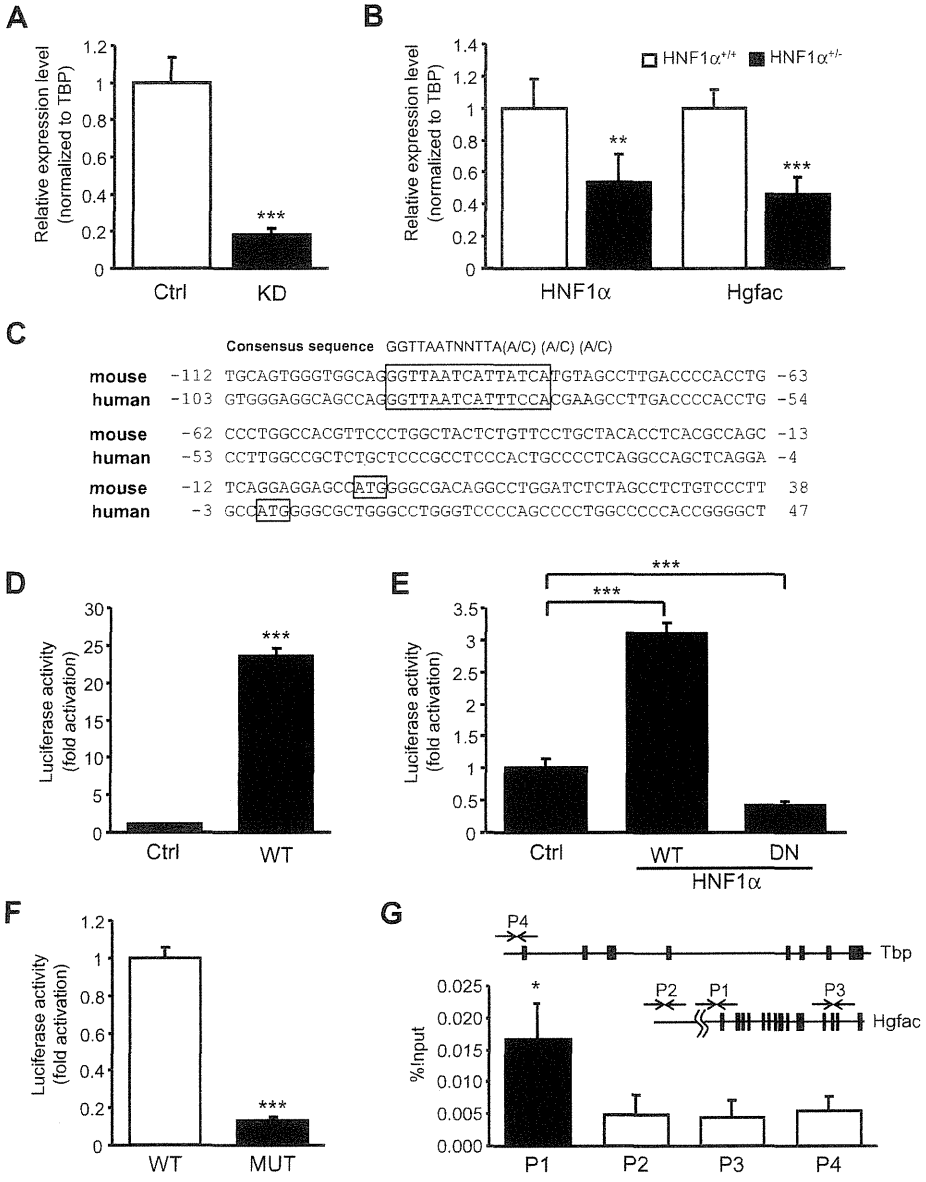

Fig. 2. Transcriptional regulation of *Hgfac* by HNF1α. (A) Expression of Hgfac mRNA by control (Ctrl) cells ($n = 3$) and HNF1α KD-MIN6 cells (KD) ($n = 3$). Expression is normalized for that of Tbp. (B) Expression of HNF1α and Hgfac mRNA in HNF1α (+/+) ($n = 4$) and HNF1α (+/−) islets ($n = 4$). (C) DNA sequences of the mouse and human Hgfac genes. The putative HNF1α-binding site is shown by a box. (D) HeLa cells were cotransfected with 800 ng of the pcDNA3.1-HNF1α expression vector as well as 200 ng of the pGL3-Hgfac reporter vector and 1 ng of pRL-TK. (E) MIN6 cells were cotransfected with 800 ng of the pcDNA3.1-HNF1α (WT) or the pcDNA3.1-P291fsinsC-HNF1α (DN) expression vector as well as 200 ng of the pGL3-Hgfac reporter vector and 0.4 ng of pRL-TK. (F) MIN6 cells were cotransfected with 800 ng of the pcDNA3.1-HNF1α (WT) expression vector as well as 200 ng of the pGL3-Hgfac (WT) or pGL3-Hgfac-mutant (MUT) reporter vector and 0.4 ng of pRL-TK. (G) Chromatin immunoprecipitation assay with MIN6 cells. PCR was performed using 4 different primer sets (P1–P4). The P2–4 regions lack the HNF1α-binding motif. Interaction of HNF1α with the P1 region of *Hgfac* was observed. Data are the mean ± SD ($^{*}p < 0.05$, $^{**}p < 0.01$, $^{***}p < 0.001$).

decline of β-cell mass, and loss of HGF signaling also accelerates the onset of diabetes in response to multiple low-dose injections of streptozotocin [21,22]. These data strongly suggest that HGF has an important influence on β-cell mass and β-cell function.

HGF is secreted in a latent form, and proteolytic conversion by the serine protease HGF activator (Hgfac) is required for its activation [14]. In this study, we found that Hgfac expression was markedly decreased in both HNF1α KD-MIN6 cells and islets from HNF1α (+/−) mice. The reporter and ChIP assays demonstrated that HNF1α bound to the conserved binding site of the *Hgfac* promoter and that it activated transcription of this gene, indicating that *Hgfac* is a direct target of HNF1α in β-cells. Although the molecular mechanisms underlying MODY3 are still unknown, HNF1α (−/−) mice and transgenic mice expressing the naturally occurring dominant negative form of human HNF1α (P291fsinsC) in their β-cells exhibit progressive reduction of β-cell mass and β-cell proliferation, indicating that HNF1α is required to maintain the β-cell mass [6,7]. Reduction of *Hgfac* gene expression and a consequent decrease of HGF signaling in β-cells might occur in HNF1α mutant mice as well as in patients with MODY3. It is possible that HNF1α controls β-cells mass at least partly by regulating cellular Hgfac expression. Investigation of β-cell specific Hgfac knockout mice could improve our understanding of how a reduction of HNF1α activity leads to a decline of β-cell mass and the onset of diabetes.

In conclusion, we established a novel cellular model of MODY3, HNF1α KD-MIN6 cells, and we identified many genes that were down-regulated in these cells. Further investigation of HNF1α KD-MIN6 cells could be useful to identify novel target genes of HNF1α in β-cells.

Acknowledgments

We thank Prof. Miyazaki (Osaka University) for the kind gift of MIN6 cells, and Prof. T. Kitamura (Tokyo University) for providing Plat-E cells. This work was supported by a Grant-in-Aid for Scientific Research (S), a Grant-in-Aid for Scientific Research on Innovative Areas, Health Labour Sciences Research Grant, and Grants from the Takeda Science Foundation, Novo Nordisk Insulin Research Foundation, Banyu Life Science Foundation International, and Japan Diabetes Foundation.

Appendix A. Supplementary data

Supplementary data associated with this article can be found, in the online version, at http://dx.doi.org/10.1016/j.bbrc.2012.07.134.

References

[1] D.B. Mendel, G.R. Crabtree, HNF-1, a member of a novel class of dimerizing homeodomain proteins, J. Biol. Chem. 266 (1991) 677–680.
[2] T. Nammo, K. Yamagata, R. Hamaoka, Q. Zhu, T. Akiyama, F. Gonzalez, J. Miyagawa, Y. Matsuzawa, Expression profile of MODY3/HNF-1α protein in the developing mouse pancreas, Diabetologia 45 (2002) 1142–1153.
[3] M. Frain, G. Swart, P. Monaci, A. Nicosia, S. Stilmpfli, R. Frank, R. Cortese, The liver-specific transcription factor LF-B1 contains a highly diverged homeobox DNA binding domain, Cell 59 (1989) 145–157.
[4] K. Yamagata, N. Oda, P.J. Kaisaki, S. Menzel, H. Furuta, M. Vaxillaire, L. Southam, R.D. Cox, G.M. Lathrop, V.V. Boriraj, X. Chen, N.J. Cox, Y. Oda, H. Yano, M.M. Le Beau, S. Yamada, H. Nishigori, J. Takeda, S.S. Fajans, A.T. Hattersleystar, N. Iwasaki, T. Hansen, O. Pedersen, K.S. Polonsky, R.C. Turner, G. Velho, J-C. Chèvreparallel, P. Froguel, G.I. Bell, Mutations in the hepatocyte nuclear factor-1α gene in maturity-onset diabetes of the young (MODY3), Nature 384 (1996) 455–458.
[5] M.M. Byrne, J. Sturis, S. Menzel, K. Yamagata, S.S. Fajans, M.J. Dronsfield, S.C. Bain, A.T. Hattersley, G. Velho, P. Froguel, G.I. Bell, K.S. Polonsky, Altered insulin secretory responses to glucose in diabetic and nondiabetic subjects with mutations in the diabetes susceptibility gene MODY3 on chromosome 12, Diabetes 45 (1996) 1503–1510.
[6] M. Pontoglio, S. Sreenan, M. Roe, W. Pugh, D. Ostrega, A. Doyen, A.J. Pick, A. Baldwin, G. Velho, P. Froguel, M. Levisetti, S. Bonner-Weir, G.I. Bell, M. Yaniv, K.S. Polonsky, Defective insulin secretion in hepatocyte nuclear factor 1α-deficient mice, J. Clin. Invest. 101 (1998) 2215–2222.
[7] K. Yamagata, T. Nammo, M. Moriwaki, A. Ihara, K. Iizuka, Q. Yang, T. Satoh, M. Li, R. Uenaka, K. Okita, H. Iwahashi, Q. Zhu, Y. Cao, A. Imagawa, Y. Tochino, T. Hanafusa, J. Miyagawa, Y. Matsuzawa, Mutant hepatocyte nuclear factor-1α in pancreatic β-cells causes abnormal islet architecture with decreased expression of E-cadherin, reduced β-cell proliferation, and diabetes, Diabetes 51 (2002) 114–123.
[8] K. Yamagata, Q. Yang, K. Yamamoto, H. Iwahashi, J. Miyagawa, K. Okita, I. Yoshiuchi, J. Miyazaki, T. Noguchi, H. Nakajima, M. Namba, T. Hanafusa, Y. Matsuzawa, Mutation P291fsinsC in the transcription factor hepatocyte nuclear factor-1α is dominant negative, Diabetes 47 (1998) 1231–1235.
[9] H. Wang, P. Maechler, K.A. Hagenfeldt, C.B. Wollheim, Dominant-negative suppression of HNF-1α function results in defective insulin gene transcription and impaired metabolism-secretion coupling in a pancreatic β-cell line, EMBO J. 17 (1998) 6701–6713.
[10] S.F. Boj, M. Parrizas, M.A. Maestro, J. Ferrer, A transcription factor regulatory circuit in differentiated pancreatic cells, Proc. Natl. Acad. Sci. USA 98 (2001) 14481–14486.
[11] K. Fukui, Q. Yang, Y. Cao, N. Takahashi, H.H. Atakeyama, H. Wang, J. Wada, Y. Zhang, L. Marselli, T. Nammo, K. Yoneda, M. Onishi, S. Higashiyama, Y. Matsuzawa, F.J. Gonzalez, G.C. Weir, H. Kasai, I. Shimomura, J. Miyagawa, C.B. Wollheim, K. Yamagata, The HNF-1 target collectrin controls insulin exocytosis by SNARE complex formation, Cell Metab. 2 (2005) 373–384.
[12] P. Akpinar, S. Kuwajima, J. Krützfeldt, M. Stoffel, Tmem27: a cleaved and shed plasma membrane protein that stimulates pancreatic beta cell proliferation, Cell Metab. 2 (2005) 385–397.
[13] J.M. Servitja, M. Pignatelli, M.A. Maestro, C. Cardalda, S.F. Boj, J. Lozano, E. Blanco, A. Lafuente, M.I. McCarthy, L. Sumoy, R. Guigó, J. Ferrer, Hnf1α (MODY3) controls tissue-specific transcriptional programs and exerts opposed effects on cell growth in pancreatic islets and liver, Mol. Cell Biol. 29 (2009) 2945–2959.
[14] K. Miyazawa, Hepatocyte growth factor activator (HGFA): a serine protease that links tissue injury to activation of hepatocyte growth factor, FEBS J. 277 (2010) 2208–2214.
[15] J. Miyazaki, K. Araki, E. Yamato, H. Ikegami, T. Asano, Y. Shibasaki, Y. Oka, K. Yamamura, Establishment of a pancreatic beta cell line that retains glucose-inducible insulin secretion: special reference to expression of glucose transporter isoforms, Endocrinology 127 (1990) 126–132.
[16] T. Kitamura, Y. Koshino, F. Shibata, T. Oki, H. Nakajima, T. Nosaka, H. Kumagai, Retrovirus-mediated gene transfer and expression cloning: powerful tools in functional genomics, Exp. Hematol. 31 (2003) 1007–1014.
[17] Y. Sato, M. Hatta, M.F. Karim, T. Sawa, F.Y. Wei, S. Sato, M.A. Magnuson, F.J. Gonzalez, K. Tomizawa, T. Akaike, T. Yoshizawa, K. Yamagata, Anks4b, a novel target of HNF4α protein interacts with GRP78 protein and regulates endoplasmic reticulum stress-induced apoptosis in pancreatic β-cells, J. Biol. Chem. 287 (2012) 23236–23245.
[18] S.F. Boj, D. Petrov, J. Ferrer, Epistasis of transcriptomes reveals synergism between transcriptional activators Hnf1α and Hnf4α, PLoS Genetics 6 (2010) e1000970.
[19] T. Nakamura, T. Nishizawa, M. Hagiya, T. Seki, M. Shimonishi, A. Sugimura, K. Tashiro, S. Shimizu, Molecular cloning and expression of human hepatocyte growth factor, Nature 342 (1989) 440–443.
[20] A. Garcia-Ocaña, K.K. Takane, M.A. Syed, W.M. Philbrick, R.C. Vasavada, A.F. Stewart, Hepatocyte growth factor overexpression in the islet of transgenic mice increases beta cell proliferation, enhances islet mass, and induces mild hypoglycemia, J. Biol. Chem. 275 (2000) 1226–1232.
[21] J. Mellado-Gil, T.C. Rosa, C. Demirci, J.A. Gonzalez-Pertusa, S. Velazquez-Garcia, S. Ernst, S. Valle, R.C. Vasavada, A.F. Stewart, L.C. Alonso, A. Garcia-Ocan-a, Disruption of hepatocyte growth factor/c-Met signaling enhances pancreatic beta-cell death and accelerates the onset of diabetes, Diabetes 60 (2011) 525–536.
[22] C. Demirci, S. Ernst, J.C. Alvarez-Perez, T. Rosa, S. Valle, V. Shridhar, G.P. Casinelli, L.C. Alonso, R.C. Vasavada, A. García-Ocana, Loss of HGF/c-Met signaling in pancreatic β-cells leads to incomplete maternal β-cell adaptation and gestational diabetes mellitus, Diabetes 61 (2012) 1143–1152.

FEBS Letters 586 (2012) 4215–4222

FEBS Letters

journal homepage: www.FEBSLetters.org

Novel function of transthyretin in pancreatic alpha cells

Yu Su [a], Hirofumi Jono [a,e,f,*], Yohei Misumi [b], Takafumi Senokuchi [c], Jianying Guo [a], Mitsuharu Ueda [a], Satoru Shinriki [a], Masayoshi Tasaki [a], Makoto Shono [a], Konen Obayashi [a], Kazuya Yamagata [d], Eiichi Araki [c], Yukio Ando [a]

[a] Department of Diagnostic Medicine, Graduate School of Medical Sciences, Kumamoto University Hospital, Kumamoto, Japan
[b] Department of Neurology, Graduate School of Medical Sciences, Kumamoto University Hospital, Kumamoto, Japan
[c] Department of Metabolic Medicine, Graduate School of Medical Sciences, Kumamoto University Hospital, Kumamoto, Japan
[d] Department of Medical Biochemistry, Graduate School of Medical Sciences, Kumamoto University Hospital, Kumamoto, Japan
[e] Department of Clinical Pharmaceutical Sciences, Graduate School of Pharmaceutical Sciences, Kumamoto University, Japan
[f] Department of Pharmacy, Kumamoto University Hospital, Kumamoto, Japan

ARTICLE INFO

Article history:
Received 13 September 2012
Revised 4 October 2012
Accepted 16 October 2012
Available online 26 October 2012

Edited by Ned Mantei

Keywords:
Transthyretin
Glucagon
Pancreas
Pancreatic alpha cell
Glucose homeostasis

ABSTRACT

Although transthyretin (TTR) is expressed in pancreatic alpha (glucagon) cells in the islets of Langerhans, the function of TTR in pancreatic alpha cells remains unknown. In this study, by using TTR knockout (TTR KO) mice, we determined the novel role of TTR in glucose homeostasis. We demonstrated that TTR KO mice evidenced impaired recovery of blood glucose and glucagon levels. Lack of TTR induced significantly lower levels of glucagon in the islets of Langerhans. These results suggest that TTR expressed in pancreatic alpha cells may play important roles in glucose homeostasis via regulating the expression of glucagon.

1. Introduction

Glucagon, a peptide hormone of 29 amino acids, is synthesized in and secreted from pancreatic alpha cells of the islets of Langerhans in response to mixed nutrient meals, administration of oral or intravenous (i.v.) amino acids, activation of the autonomic nervous system, and hypoglycemia [1,2]. The main action of glucagon is to raise blood glucose levels in response to hypoglycemia by increasing hepatic glycogenolysis and gluconeogenesis [3]. The circulating half-life of immunoreactive glucagon in humans is estimated to be between 5 and 6 min [4]. It is well known that the balance between insulin and glucagon controls glucose homeostasis [5]. Thus, the primary role of glucagon is correcting hypoglycemia caused by malnutrition, fasting, and treatment of diabetes to achieve normoglycemia [6–9]. Insulin treatment in diabetes, especially type 1 diabetes, greatly increases the risk of hypoglycemia, with effects on a number of organs including brain, and causes critical systemic symptoms such as hypoglycemic coma [10–12]. In addition, an absent glucagon response plays a prominent role in a failure to correct hypoglycemia induced by insulin and may exacerbate critical systemic symptoms [8]. Therefore, tight control of glucagon secretion has significant implications for stable glucose homeostasis.

Transthyretin (TTR) is a functional plasma protein, which forms a tetramer composed of four identical subunits, and serves as a transport protein for thyroxine in association with retinol-binding protein [13]. TTR is synthesized predominantly by the liver, which is therefore the main source of TTR in plasma [14,15]. It is well-documented that plasma TTR levels are reduced in inflammatory conditions and in malnutrition caused by surgery or chronic diseases [16–19]. However, TTR is expressed in considerable amounts in the choroid plexus, retinal pigment epithelium, pancreatic alpha and beta cells, although the function of TTR synthesized by these particular cells is largely unknown [20–24]. Certain studies reported a significantly lower plasma TTR level in diabetic patients than in non-diabetic subjects [25,26]. Moreover, in islet beta cells of the pancreas, TTR promoted insulin stimulus-secretion coupling and protected against beta cell apoptosis in type 1 diabetes [27]. In addition, TTR has been shown to be normally expressed in

Abbreviations: qRT-PCR, real-time quantitative RT-PCR; TTR, transthyretin; TTR KO, transthyretin knockout; WT, wild-type; ITT, insulin tolerance test

* Corresponding author. Address: Department of Diagnostic Medicine, Graduate School of Medical Sciences, Kumamoto University, 1-1-1 Honjo, Kumamoto 860-8556, Japan. Fax: +81 96 373 5283.

E-mail address: hjono@fc.kuh.kumamoto-u.ac.jp (H. Jono).

0014-5793/$36.00
http://dx.doi.org/10.1016/j.febslet.2012.10.025